UNIVERSIDAD NACIONAL AUTÓNOMA DE MÉXICO
PROGRAMA DE MAESTRÍA Y DOCTORADO EN INGENIERÍA
CENTRO DE INVESTIGACIÓN EN ENERGÍA

ENFRIAMIENTO RADIATIVO

TESIS

QUE PARA OPTAR POR EL GRADO DE

MAESTRO EN INGENIERÍA

P R E S E N T A:

JOSÉ ÁNGEL ARANDA MORALES

DIRECTOR DE TESIS:

DR. JORGE ROJAS MENÉNDEZ
Instituto de Energías Renovables

Temixco, Morelos. Agosto 2013

JURADO ASIGNADO:

Presidente	Dr. Roberto Best y Brown
Secretario	Dr. Jorge Rojas Menndez
Vocal	Dra. Guadalupe Huelz Lesbros
1er. Suplente	Dr. Sergio Cuevas Garca
2o. Suplente	Dra. María Guadalupe Alpuche Cruz

Lugar donde se realizó la tesis:

Instituto de Energías Renovables - UNAM

DIRECTOR DE TESIS:
Dr. Jorge Rojas Menéndez

_____
FIRMA

Acknowledgments

To the National University of Mexico UNAM, particularly to the Institute of Renewable Energy IER for this great opportunity.

To CONACyT and Fomix CONACyT Morelos project 93693 for its financial aid.

To everyone in the Refrigeration Laboratory, specially to Dr. Jorge Hernández for his guidanceand counsel; Emmanuel Salazar and Roy Solano for their collaboration everyday during experimentation hours. Also to Guillermo Hernández in the Thermalscience Lab

Every member of the jury.

Greatly to Jorge Rojas for letting me work beneath his tutorship and guiding my academic development.

To my loving parents, Agustn and Clara, for their unconditional support; and my brothers Ana, Abel, and Agustn, for their cheering and encouragement.

Also, to all my fellow students for sharing with me those long hours of study.

Contents

Resumen

Este documento presenta un estudio de validación de un panel para enfriamiento radiativo bajo condiciones climáticas propias al territorio mexicano. El panel fue construido e instalado en una sala de cómputo ubicada en el laboratorio de refrigeración del *Centro de Investigación en Energía* en Temixco, Morelos. Dicho panel consiste en un conjunto de tubos plásticos distribuidos en las superficies de la habitación por los que circula agua a baja temperatura. De esta manera se favorece la transferencia de calor por radiación entre las cargas térmicas de la habitación y el fluido de trabajo. La intención de este intercambio de calor es alcanzar una sensación de confort térmico en los usuarios de la sala. Distintos parámetros fueron medidos y analizados para ser comparados a los resultados de un modelo virtual en condiciones similares a través del software *EnergyPlus*. Una vez validados los resultados del software, se varió el funcionamiento del panel radiativo para identificar las características importantes del sistema y proponer condiciones de mejor desempeño y el eventual acoplamiento a otros sistemas de climatización.

Abstract

This document presents a study of a radiant panel used for cooling under climatic conditions of Mexico. The radiant panel was built and installed in a computer room located in the Refrigeration Lab in the *Centro de Investigación en Energía* (Energy Research Center) in Temixco, Morelos. This panel consists of a group of plastic tubes, distributed through the room's surfaces, in which chilled water is circulated. In this way, heat transfer by radiation takes place between the room's surfaces and the panel, and then to the working fluid by conduction. The heat transfer is meant to achieve thermal comfort of inhabitants. Several parameters were sensed and analyzed to be compared with a virtual model developed using *EnergyPlus* software. Once the simulation results were validated, different operation conditions of the radiant panel were tested to identify important characteristics of the system and propose better performance conditions and a future coupling with other conditioning systems.

Introduction

Energy efficiency has become a worldwide concern in recent years. The living style that industrialized countries have adopted will not be able to be maintained unless radical changes concerning energy generation and consumption take over. The high dependence on hydrocarbon and non-renewable fuels has lead to economic and social crisis.
According to the *International Energy Agency*, in 2010 more than 80% of the total primary energy supply came from coal, oil, and natural gas [**?**]. Excluding transportation, around 40% of the energy ends up in commercial and residential sectors. In a developed country, such as the United States, the energy consumed for space conditioning in buildings is roughly 1.96 quads BTU per year (approximately 64.66 GWy) [**?**].
Working towards an increase in systems efficiency and a decrease in energy consumption could mean the difference between an energetic crisis and a reinvention of the world's society. This is the core motivation of the present work; finding an alternative to high energy consuming HVAC systems without giving up the comfort of the modern men culture can aid that purpose.
A single project could not resolve the energetic issues, but it is part of the answer to an essential necessity; and working on a key branch of the energy's transformation path brings us a step closer to that answer.
As previously stated, comfort has become a requirement to contemporary men and women. A big part of their resources are destined to their thermal comfort. In the succeeding pages, chilled radiant panels are proposed as an auxiliary or even a supplementary system to conventional air conditioning systems. These chilled systems will be applied particularly to warm sub-humid climatic conditions, such as those prevailing in the low central regions of Mexico.
Creating and improving climatic information as well as introducing useful new tools to Mexico's academic environment is also an important purpose of this work.
The present endeavor comprehends the construction of a radiant panel with components available and easily accessible in the area. Afterwards, installed and instrumented in a computing room of a laboratory facility. In like manner, a equivalent computing room equipped with a radiant system is created using CAD software *DesignBuilder* and then exposed to the same climatic conditions through *EnergyPlus* simulating program. The simulations are set to throw the same data as the sensors installed in the actual room to be compared. By doing this, the software simulation is intended to be validated as a fair model of the radiant system's performance, as well as the local weather conditions and construction systems.

Chapter 1

Background

A better understanding and consequently a better design will be achieved by the examination of the physical phenomena involved in radiant devices. Radiant heat transfer, thermal comfort notions, and low energy conditioning strategies are crucial elements along this work.

1.1 Radiant Heat Transfer

1.1.1 General Concepts

Heat transference by thermal radiation, unlike conduction or convection, does not require matter as a mean of transmission. We associate thermal radiation with the rate at which energy is emitted by matter as a result of its finite temperature. The mechanism of emission is related to the energy released as a result of oscillations of the many electrons that constitute matter. These oscillations are sustained by the internal energy, and therefore temperature, of the matter [**?**, **?**].
All kinds of matter emit radiation. Nevertheless, most radiation emitted in the interior of solids and liquids is absorbed by adjacent molecules, except on the surface; consequently, radiation in solids and liquids is considered a surface phenomenon.
Therefrom, radiation can also be viewed as the propagation of electromagnetic waves, and as such, a frequency (ν) and a wavelength (λ) can be designated. Each wavelength can then be associated to a temperature. In the electromagnetic spectrum, thermal heat transfer is comprehended in the areas of ultraviolet, visible, and infrared waves; that is between 0.1 and 100 μm [**?**].
Radiation coming from a body's surface is emitted in all possible directions. The magnitude of the radiation can vary according to its wavelength or spectral distribution, and its directional distribution. To find out the magnitude of energy transmitted by a body, a volumetric integration that depends on each of these variables needs to be calculated

$$E_\lambda = \int_0^{2\pi} \int_0^{\pi/2} I_{\lambda,e}(\lambda, \theta, \phi) \cos\theta \sin\theta d\theta d\phi \tag{1.1}$$

where the spectral intensity $I_{\lambda,e}$ is the rate at which radiant energy is emitted at the wavelength λ in the (θ, ϕ) direction (in spherical coordinates), per unit area of the emitting surface normal to this direction, per unit solid angle about this direction, and per unit wavelength interval $d\lambda$ about λ. As it can be observed, the spectral intensity is integrated in the semi-sphere surrounding the emitting surface (see Figure **??**) [**?**].

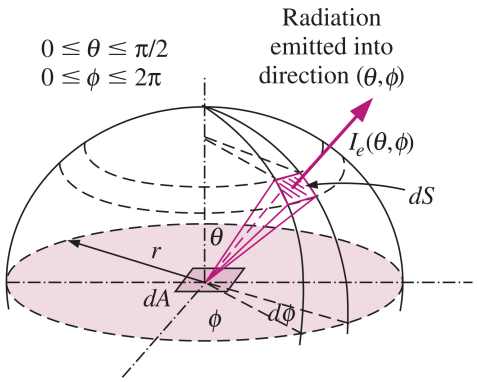

Figure 1.1: Emission of radiation into the surrounding hemispherical space.

If the emissive power per area is integrated throughout all the possible wavelengths, then the total hemispherical emissive power is

$$E = \int_0^\infty E_\lambda(\lambda) d\lambda \tag{1.2}$$

However, the concept of *blackbody* is used to simplify the calculations. A *blackbody* is an ideal surface that absorbs all incident radiation, emits the most possible radiation for a specific temperature and wavelength, and it is a diffuse emitter, i.e. it emits in every direction.
Max Planck determined the spectral distribution of blackbody emission (see Figure **??**) and was able to figure important characteristics:

- Emitted radiation varies with wavelength.
- The magnitude of emitted radiation increases with increasing temperature for a given wavelength.
- Temperature dictates the spectral region in which radiation is concentrated.
- Comparatively more radiation appears at shorter wavelengths as the temperature increases.

Following the integration to Planck's spectral body distributions made by Josef Stefan and Ludwig Boltzmann, it can be shown that the emissive power of a blackbody is

$$E_b = \sigma T^4 \tag{1.3}$$

where it is determined that $\sigma = 5.670 \times 10^{-8}\ W/m^2K^4$. Equation **??** is known as the *Stefan-Boltzmann Law*.
Real surfaces define their emissivity (ϵ) as the ratio of radiation emitted by the surface and that emitted by a blackbody at the same temperature. Nevertheless, emissivity can also be affected by spectral and directional distribution. Typical ranges of emissivity for different materials can be referred in Figure **??**.

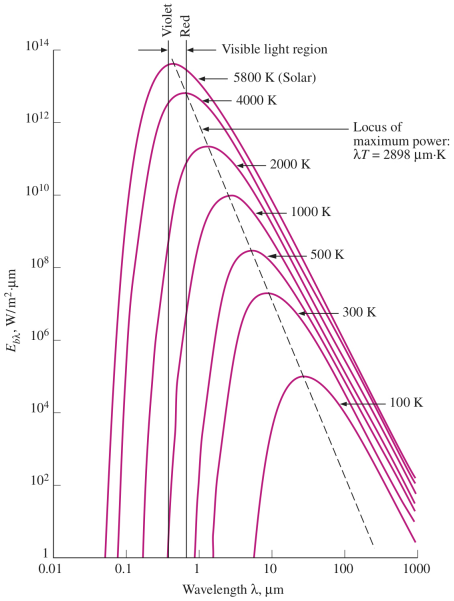

Figure 1.2: Spectral distribution emission of a blackbody determined by Max Planck.

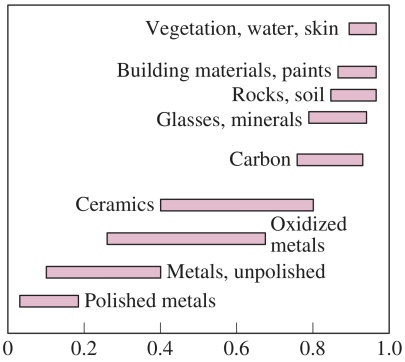

Figure 1.3: Typical ranges of emissivity for various materials.

1.1.2 View Factor

To evaluate the heat exchange between two bodies, in addition to the amount of energy that leaves the first, it is necessary to take into account the energy that is received by the second. The energy flux received by a surface in any direction is known as *irradiation* [**?**]. In this case, it is to be assessed the amount of irradiation coming from a room occupant (and/or thermal loads) that is collected by the radiant panel.
The irradiated amount of energy largely depends in the position of both surfaces: put in other words, it is the way one surface *sees* the other surface, how much of its view is occupied by the irradiated surface. This geometric relations between exchanging surfaces are known by many names: *view factor, configuration factor, angle factor, shape factor* [**?**]. The view factor between two surfaces A_i and A_j is defined as

$$F_{i-j} \equiv \frac{\text{diffuse energy leaving } A_i \text{ directly toward and intercepted by } A_j}{\text{total diffuse energy leaving } A_i} \tag{1.4}$$

Even though view factors are simple geometric relations, working in a three-dimensional environment with many surfaces complicates considerably the calculations. Radiation view factors obtained by *EnergyPlus* are solved by numeric methods with an auxiliary package called *View3D* that feeds the simulator data with a convergence of 1.0×10^{-4} [**?**]. Emissivity (ϵ) and the view factor (F_{i-j}) are important elements that both describe and prescribe radiant heat transfer.
As it has been stated and seen in the equations of *Stefan-Boltzmann Law*, radiant heat transfer does not need matter as a medium. This means that, while a temperature difference prevails between two bodies, the heat transfer will continue to occur. In this particular project, the bodies of interest are the radiant panel and the room's occupiers. If the radiative heat transfer between these entities is properly achieved, thermal comfort of the users may be resolved.

1.2 Thermal Comfort

Thermal comfort is defined by norm ISO 7730 as *that condition of mind which expresses satisfaction with the thermal environment* [**?**]. Translating this into physically measurable values is a very difficult task. Thermal comfort depends on air temperature, radiant temperature, humidity, wind velocity, clothing, metabolic stimulation, and even biological and cultural adaptation [**?**]. Reaching a general value for thermal comfort would be virtually impossible. However, PMV index (Predicted Mean Vote) predicts the mean value of comfort sensation in a group of people. Developed by P. Ole Fanger, the PMV index sets a range, between -3 (cold) to 3 (hot), where zero means thermal comfort. The PMV was developed by collecting opinions among users of a temperature-controlled room and identifying the aspects involved in a person's thermal regulation. Those factors were then given a factor of weight. The PMV is calculated with the next equations:

$$PMV = [0.303e^{-0.036M} + 0.028]\{(M - W) - 3.05 \times 10^{-3}[5773 - 6.99(M - W) - p_a] - 0.420[(M - W) - 58.15] - 1.7 \times 10^{-5}M(5867 - p_a) - 0.0014M(34 - t_a) - 3.96 \times 10^{-8}f_{cl}[(t_{cl} + 273)^4 - (\bar{t}_r + 273)^4] - f_{cl}h_c(t_{cl} - t_a)\} \quad (1.5)$$

$$t_{cl} = 35.7 - 0.028(M - W) - I_{cl}\{3.96 \times 10^{-8}f_{cl}[(t_{cl} + 273)^4 - (\bar{t}_r + 273)^4] + f_{cl}h_c(t_{cl} - t_a)\} \quad (1.6)$$

$$h_c = \begin{cases} 2.38|t_{cl} - t_a| & \text{for } 2.38|t_{cl} - t_a|^{0.25} > 12.1\sqrt{v_{ar}} \\ 12.1\sqrt{v_{ar}} & \text{for } 2.38|t_{cl} - t_a|^{0.25} < 12.1\sqrt{v_{ar}} \end{cases} \quad (1.7)$$

$$f_{cl} = \begin{cases} 1.00 + 1.29I_{cl} & \text{for } I_{cl} \leqslant 0.078\frac{m^2K}{W} \\ 1.05 + 0.645I_{cl} & \text{for } I_{cl} > 0.078\frac{m^2K}{W} \end{cases} \quad (1.8)$$

where the meaning of each variable is:

M	metabolic rate in W/m^2
W	effective mechanical power in W/m^2
I_{cl}	clothing insulation in m^2K/W
f_{cl}	clothing surface area factor
t_a	air temperature in $°C$
$\bar{t}_r$	mean radiant temperature in $°C$
v_{ar}	relative air velocity in m/s
p_a	water vapor partial pressure in Pa
h_c	convective heat transfer coefficient in $W/(m^2K)$
t_{cl}	clothing surface temperature in $°C$

Typical values for metabolic rate (M), effective mechanical power (W), and clothing insulation (I_{cl}) can be found in tables in ISO 7730; calculation methods can be consulted in norms ISO 8996 and ISO 9920 [**?**].
Air temperature (t_a), relative air velocity (v_{ar}), water vapor partial pressure (p_a), and clothing surface temperature (t_{cl}) need to be measured. The mean radiant temperature ($\bar{t}_r$) is defined as the uniform temperature of an imaginary enclosure in which the radiant heat transfer from the human body is equal to the radiant heat transfer in the actual non-uniform enclosure [**?**]. Mean Radiant temperature can be calculated by

$$\bar{t}_r = \sqrt[4]{\sum_n F_{i-j}(t_i + 273)^4} - 273 \quad (1.9)$$

where t_i is the temperature of the i-surface and F_{i-j} is the view factor between the occupant and the i-surface. As previously mentioned, view factors calculation can complicate greatly the estimations. A simpler approximation can be achieved by measuring the air temperature (t_a) and the globe temperature (t_g); for the latter a black globe thermometer is needed, such as the one described in section **??**. Then equation **??** can be replaced with

$$\bar{t}_r = \sqrt[4]{(t_g + 273)^4 + \frac{h_{cg}}{h_r}(t_g - t_a)} - 273 \tag{1.10}$$

Where the radiant (h_r) and globe convection (h_{cg}) coefficients are

$$h_r = 5.38 \times 10^{-8} \tag{1.11}$$

$$h_{cg} = \begin{cases} 6.3\dfrac{v_a^{0.6}}{D^{0.4}} & \text{for forced convection} \\ 1.4\left(\dfrac{|t_g - t_a|}{D}\right)^{0.25} & \text{for free convection} \end{cases} \tag{1.12}$$

D stands for the globe's diameter. The mean radiant temperature must be taken into account while comfort calculations are made; the temperature that a person perceives is a combination of the dry bulb air temperature and the radiant temperature, referred as the operative temperature (t_o). Thermal comfort can be achieved dealing with these temperatures; radiant heat exchange enhanced by a chilled radiant panel will affect the temperature observed by a person, bringing him/her closer to the comfort zone in a warm environment.

ASHRAE Handbook Fundamentals proposes a method for radiant temperature calculations from planar temperatures in six directions (up, down, left, right, front, back) which would form an equivalent envelope taking into account the projected view factors of those planes [**?**]. Mean radiant temperature may be estimated as

$$\bar{t}_r = \frac{0.08[t_p(up) + t_p(down)] + 0.23[t_p(right) + t_p(left)] + 0.35[t_p(front) + t_p(back)]}{2(0.08 + 0.23 + 0.35)} \tag{1.13}$$

where t_p is the planar temperature. The planar temperature is defined as the uniform temperature of an enclosure in which the incident radiant flux on one side of a small plane element is the same as that in the actual environment [**?**]; so the mean radiant temperatures of an equivalent envelope was calculated using inside surface temperatures of each wall in the *test room*. Figures **??** through **??** show the radiant temperature calculated with ASHRAE method using planar temperatures, both experimental and simulated.

P. Ole Fanger graphed a comfort diagram based on his calculations showing the combined influence of mean radiant temperature and air temperature [**?**]. In Figure **??** comfort lines are shown for different mean air velocities, applied on people with sedentary activities (1.0 MET) and medium clothing (1.0 CLO).

Another diagram, found in the ASHRAE Handbook Fundamentals, presents a range of conditions that form a comfort zone for warm and cool seasons, see Figure **??**. This

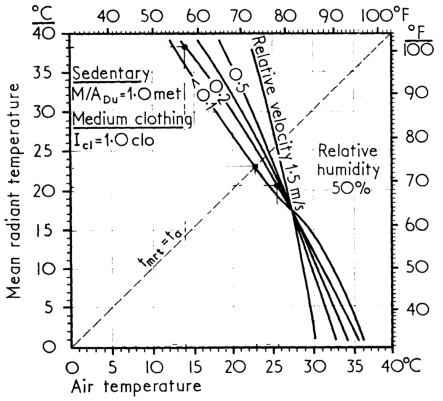

(a) P.O. Fanger comfort diagram which relates radiant and air temperature, valid for sedentary activities and 50% relative humidity.

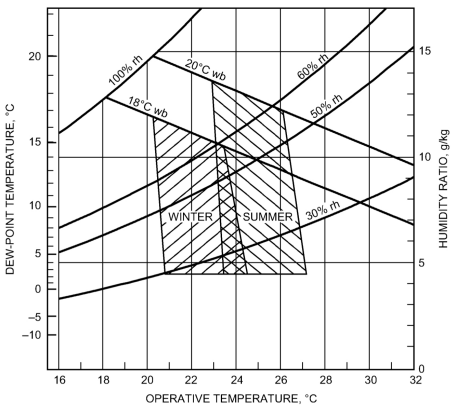

(b) ASHRAE Handbook Fundamentals comfort zone for summer and winter conditions.

Figure 1.4: Comfort Diagrams.

comfort diagram uses the operative temperature t_o which is the average of the mean radiant and air temperatures, weighed by their heat transfer coefficients h_c and h_r; the former being the convective coefficient heat transfer in $W/(m^2K)$ latter being the linear radiative heat transfer coefficient in $W/(m^2K)$ [**?**].

$$t_o = \frac{h_r \bar{t}_r + h_c t_a}{h_r + h_c} \tag{1.14}$$

For occupants engaged in sedentary activities (1.0 to 1.3 MET), not in direct sunlight, and not exposed to air velocities greater than 0.20 m/s, the relationship can be approximated with [**?**]

$$t_o = \frac{\bar{t}_r + t_a}{2} \tag{1.15}$$

An adaptive model of human thermal comfort, based on a compilation of past studies and models performed in several cities around the world, proposes an operative comfort temperature set point for rooms where cooling and central heating is not present [**?**], recommended also in ASHRAE Fundamentals Handbook. Being t_{out} the monthly mean outdoors temperature

$$t_{oc} = 18.9 + 0.255 t_{out} \tag{1.16}$$

Since t_{out} can be calculated directly from the weather station data, this operative comfort temperature will serve as reference of the panel's performance. Also, according to ASHRAE Fundamentals Handbook, the comfort temperature is likely to increase with the freedom to adapt given to the occupants.

1.3 Low Power Conditioning Strategies

Several architectural ideas are being rediscovered by contemporary architects; most vernacular constructions all around the world enhance thermal comfort with passive strategies that seize particular climatic characteristics of the site. Such strategies are now being adapted to modern buildings to provide cooling and heating without the total dependence of conventional energy supplies. In general, these conditioning strategies can be classified in the following kinds [**?**].

- *Typology.* A building construction can be assessed by its compactness, which is the ratio between its volume and its total exterior surface; the higher the ratio, the lower conditioning energy will be demanded.
- *Orientation.* Sunshine can be both desirable or disadvantaging, depending on the overall weather conditions. A building in cooler climates can exploit those thermal gains, while it would be inappropriate for warmer climates constructions. Solar heat gains can be managed through the building's orientation.
- *Shading.* Solar protection can minimize the cooling demand in a room. In places where season temperatures changes are considerable, a precise design can offer protection only during hot seasons and allow solar gains during cold seasons.
- *Thermal Mass.* In places with substantial fluctuations in day and night temperatures, it is convenient to build with materials that can absorb and store thermal energy. One of such materials could store energy captured from solar radiation and release it during the night when temperatures drop.
- *Natural Ventilation.* Creating pressure differences through openings layout can enhance an airflow that could mean better indoor air quality, cooler temperatures, and wind.
- *Night Ventilation.* With lower nocturnal temperatures, outside air can be used to pre-cool building spaces.
- *Evaporative Cooling.* Important amounts of energy can be lost by hot air while evaporating water, thus a cooler airflow can be achieved. In dry weather, along with cooler temperatures, air humidification can enhance thermal comfort.
- *Envelope Insulation.* Proper insulating materials will decrease heat transference by conduction between a harsh environment and the indoors.

More complex devices have been developed using these basic strategies. Available technology and natural characteristics of the site can become more effective in creating adequate conditions of temperature, humidity, wind, air quality, and a comfortable life-style: underground plenums with constant temperatures and large thermal mass help to maintain comfortable air temperatures that can be circled into occupied chambers; fountains located near ventilation paths increases the airflow freshness; water deposits that can

Figure 1.5: Radiant panel mounted inside a false ceiling (opened to show the inside).

capture solar radiation to get warm water.
These strategies, despite not being passive, require lesser amounts of energy to function than conventional conditioning systems. Although one conditioning strategy may not completely resolve thermal comfort issues, a combination of several strategies, along with a wise complement of traditional conditioning systems, will point towards a more energy-efficient construction.

1.4 Radiant Panels

A radiant panel is a low energy conditioning device. It consists of a lightweight panel installed in one or several surfaces of a room. On the back of the panel exists a series of pipes through which heated or chilled water is pumped, see Figure **??** [**?**]. Heat is transferred between the water and the visible surfaces in the room via radiation, since there is a temperature difference between the water flow and the bodies in the room [**?**]. Energy consumption of the system needed to circle chilled water through the panel's piping makes radiant panels an attractive conditioning alternative, or even an important aid to traditional systems.
A review presented by Orosa of thermal comfort models [**?**], shows that the radiant fraction of the heat transfer plays an important role in achieving comfort. This radiant effect has been experimentally tested for cooling of a residential building, with built-in hydronic panels, in desert conditions by Chantrasrisalai et. al., [**?**] and with chilling tubing embedded in the roof of a building exposed to Mediterranean weather by Dimoudi and Androutsopoulus [**?**]; the latter state the importance of the water flow rate in its effectiveness, and they both agree that more studies about configuration are needed to optimize panel's performance. Numerical models have been developed to evaluate radiant heat transfer in different tubing configurations set in a controlled environment by Okamoto et. al. [**?**], being validated experimentally; they showed that piping density has little impact on heat flux rate, but denser piping achieves more homogenous surface temperatures.

1.5 Radiant Devices in Mexico

Although hydronic radiant devices have been present since good part of the last century [**?**], it is still a relatively young technology as almost no application was materialized until fifteen years ago. In highly developed countries, radiant panels have been incorporated to new constructions. Since a radiant panel can be used for cooling as well as for heating by controlling the water temperature, they are becoming more popular in places with manifested seasons. Germany, South Korea, and afterwards the United States have become leaders in commercial hydronic radiant systems, nevertheless there is no consensus of optimal configuration or range of application of low temperature radiant systems [**?**].
There is a late start and little research in Mexico for radiant heat transference systems. Unfortunately, that is the case with most bioclimatic design topics and building efficiency regulations. Among the efforts that can have an impact on low energy conditioning devices, there exist official norms (NOM-008-ENER, NOM-020-ENER) which are an important thrust towards better and cleaner construction practices. Regrettably, poor expertise in the area have made these norms insufficient, added to almost no control and supervision of their implementation. Also, more flexible mortgages are being given to those residential constructions that count with green elements.
EnergyPlus and other software have proven to be most useful in regards of thermal energy simulations in building constructions. Still, a lack of climatic information and the great diversity of weather conditions within Mexico make it difficult to assess virtual simulations.

Chapter 2

Panel Installation

2.1 Location

The city of Temixco stands next to Cuernavaca about 80 km south of Mexico City at 18°34′59″ N 99°02′42″ W in the central state of Morelos (see Figure **??**). Its altitude is 1280.0 $m.a.s.l.$ and presents a warm sub-humid climate. It has a mean annual temperature of 23.2°C, oscillating between 30.7°C and 15.8°C, and precipitation of 903.8 mm, mainly in the spring and summer months.
Located in Temixco, the *Instituto de Energas Renovables* (IER) is a small campus of the National University of Mexico that comprises a group of offices, investigation laboratories, classrooms and auditoriums. The radiant panel was installed in the computing area of the Refrigeration Laboratory **??**.
The *test room* meets the east facade of the laboratory. It has a total floor area of 24.30 m^2 in a backwards L shape, and has the following constructions characteristics; dimensions can be seen in Figure **??**.

- *Walls and Windows:* 0.120 m brickwork with glazed areas in the west wall, plasterboard areas in the east wall, an aluminum and glass door in the north wall, and a no-glass window in the south wall communicating the computing room with the main laboratory.

- *Cover:* flat composite roof with six layers: 0.015 m of asphalt, 0.010 m of mortar, a 0.020 m layer of expanded polystyrene, 0.200 m of high density concrete, 0.200 m of an aerated concrete slab, and a 0.003 m aluminum plate.

- *Floor:* 0.100 m casted concrete slab.

The west and south walls are shared by the *test room* and the refrigeration laboratory. The north and east walls face to an outdoors hall, protected with eaves and a 1.5 m stone wall that holds a soil volume. Bamboo trees also protect the eastern face from solar radiation, as well as adjacent office buildings. In order to pursue the regular working conditions, the *test room* continued having its regular occupation and usage during the retrieval of experimental data of the panel's performance.

2.2 Thermal Loads

The computing area harbors personal computers, laptops, printers, lighting, office furniture, and of course, laboratory personnel. In Table **??** a description of the thermal loads

Figure 2.1: IER is located South to Mexico City, in the municipality of Temixco, inside Cuernavaca's metropolitan area at 18°34′59″ N 99°02′42″ W.

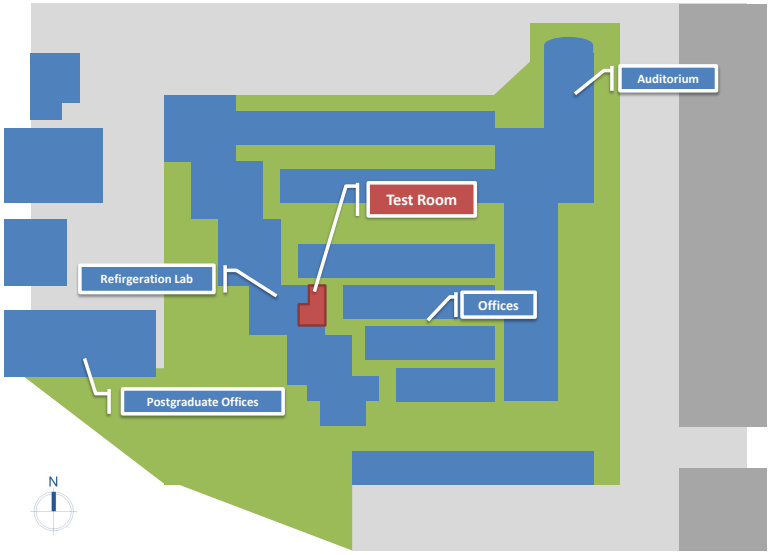

Figure 2.2: The test room (red) is part of the refrigeration lab in IER.

Thermal Loads			
Quantity	Description	Unitary Power (W)	Total Power (W)
5	Personal Computer	55	275
5	Monitor	36	180
4	Laptop	23	92
2	Printer	10	20
2	Light bulb	26	52
2	Router	5	10
1	Scanner	10	10
6	People	95	570
		Total (W)	1209

Table 2.1: Recommended heat gains values in the *Test Room* taken from AHSRAE Fundamentals [**?**].

and their consumed energy are presented [**?**].

2.3 Radiant Panel Placement

The south wall has an area of 12.90 m^2, from which 5.59 m^2 is brickwork and the remaining 7.31 m^2 is a no-glazing window that communicates with the main laboratory area. The radiant panel hangs in front of this no-glass window covering 30% of the total wall area.

2.4 Construction

The radiant panel was built with materials found in the urban area of Cuernavaca and reused parts of the IER workshops, ensuing an accessible design that can be reproduced in any location of Mexico, and conjointly achieve a lesser impact of wastes and useful life cycle.

2.4.1 Building Parts

A list of the parts used to mount the radiant panel is presented in Table **??**. Special attention is put to the parts that were readjusted to fit the system.
Due to the simplicity of the working fluid fluxes, no additional friction loses and fluid behavior were included in the study. The sizing of the tubing was chosen only to accomplish the best fit of the existing parts, such as the water tank, the radiant panel, and the water chiller. Further investigation in the regime governing the fluid dynamics escapes the span of this work.

Material		
Quantity	**Size**	**Description**
1	100 l	Water tank. Water storage tank taken from a commercial solar water heater; the only modification were the caps that sealed the cavities where the evacuated tubes are usually placed
1	1 HP	Pump
1	3 m2	Radiant Panel. A simple solar collector commonly used to heat pool water; no modifications were mad
1	1 HP	Water Chiller
1	1 1/2 in	PVC ball valve
5	1 in	PVC ball valve
5	1/2 in	PVC ball valve
2	1 in	Stainless steel globe valve
3	1 in	Stainless steel ball valve
16	1 in	Elbow tee
1	1/2 in	Elbow tee
1	1 in	45° tee
3	1 in	Tee
1	1/2 in	Tee
3	1 in	Cross Tee
2	1/2 in	Cross Tee
2	1-1/4 in	Reducer bushing
2	1-1/2 in	Reducer bushing
4	1 1/2 in	Hose 0.20 m
2	1/4 in	Hose 1.50 m
1	3/4 in	Hose 3.00 m

Table 2.2: List of parts used in the construction of the radiant panel's system. Additional fittings were attached to the piping system in order to help reparation processes, which are not listed.

2.4.2 Construction and Assembly

1. *Radiant Panel.* The radiant panel set in the *Test Room* was originally a solar heater for pools, model *PHC-40 ECOSUN*. The radiant heat exchange during experimentations is the same as its intended purpose, except for milder temperatures and environmental conditions, so no additional adaptations were needed.

2. *Water Tank.* The tank was recycled from a solar domestic water heater. The holes connecting the tank to the evacuated tubes were sealed using PVC caps and silicone. Also, the tank's stand was modified to hold the pump beneath the tank, using mounting angles.

3. *Pump.* A regular 746 W water pump was bolted to the tank's stand. A soft base absorbs part of the vibration caused by the pump.

4. *Water Chiller.* A small 1200 W chiller was set to cool the working flow.

5. *Mounting.* Using mounting angles, the radiant panel was hung vertically 1 m below the ceiling in the south wall of the *Test Room*. In the adjacent room, the water tank, pump, and chiller were placed.

6. *Connections.* All connections were made with PVC hydraulic tubing, nominally 1-inch diameter. Where the main component's connections required it, a reducer bushing was placed. Every component was connected by valves at the inlets and outlets so they could be hydraulically isolated. Water flowing from the pump passed through globe valves in order to regulate the water's flow rate.

7. *Water Circuit.* If we mark the start of the circuit in the water tank, the working fluid travels first to the pump. There it is divided in three different paths; a) into the chiller, b) through the radiant panel, or c) directly into the tank. Each of these paths return to the tank, completing the circuit. The globe valves that followed the pump into each path allowed the regulated flow rates. See Figure **??**.

2.5 Instrumentation

Necessary experimental data to be confronted with simulated data was gathered by sensing particular parameters in the radiant system and the test room: room temperatures, surface temperatures, fluid temperatures, fluid mass rate, fluid pressure, and heat flux (see Figure **??**).
All data was saved in a text file using an *Agilent 34970A Data Logger*, which can read resistance, voltage and current of different sensors in a given time interval, see Figure **??**. The readings are delivered to a computer, where a program made with *HPVEE* software transforms them into quantities with physical meaning. Certainly, previous to installation, calibration curves must be calculated for each sensor.
Room temperatures were collected using the *3M QUESTemp Heat Stress Monitor*, which

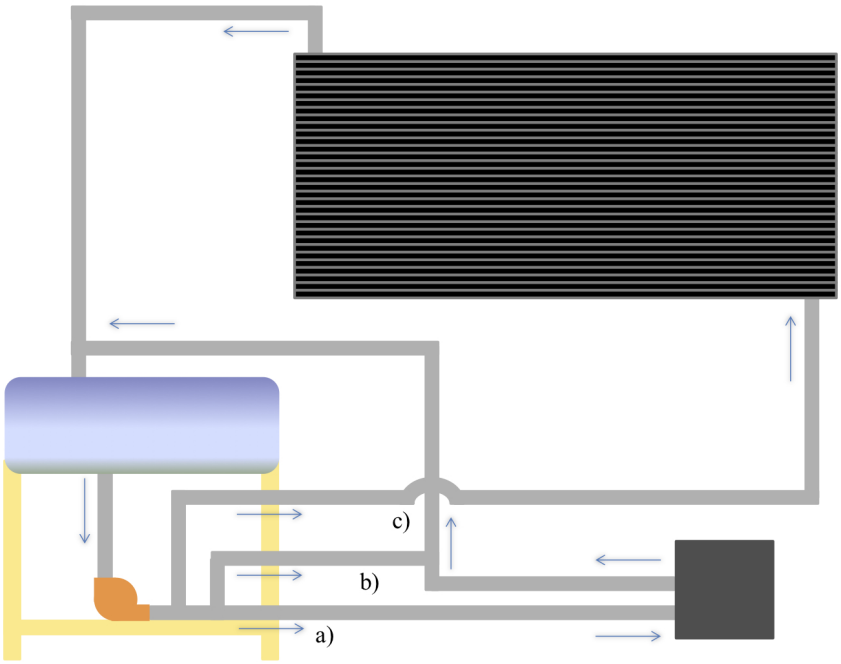

Figure 2.3: Water circuit: the working fluid travels first to the pump, there it is divided in three different paths; a) into the chiller, b) directly into the tank, or c) through the radiant panel.

(a) Data logger *Agilent 34970A*: receives sensor's information.

(b) *3M QUESTemp Heat Stress Monitor* with black globe thermometer that reads radiant temperature.

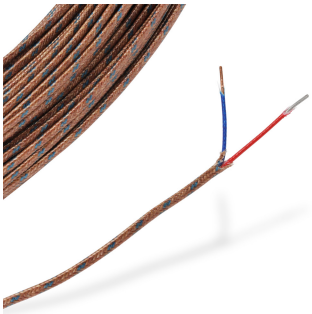

(c) Type T thermocouples

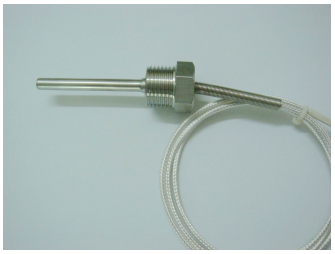

(d) PT1000 temperature sensor.

(e) Differential pressure sensor.

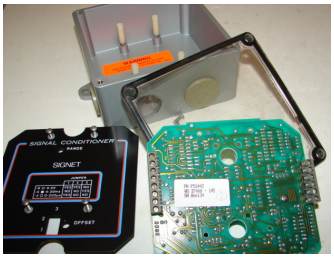

(f) *Signet Scientific MK508 Flowmeter.*

Figure 2.4: Instrumentation operating during the radiant panel system tests.

senses dry and wet bulb room temperatures, as well as black-body radiant room temperature, see Figure **??**. The monitor sensors were placed 0.40 m in front of the radiant panel surface at a height of 1.20 m.
Type T thermocouples size 24 placed on the radiant panel surface captured the temperature distribution over the surface, see Figure **??**. The same kind of thermocouples were added to the walls inner surface. Adhesive plasticine was used to fix the wires to the surfaces. Also, another thermocouple sensed the ambient room temperature to confirm the dry bulb temperature the *3M QUESTemp* reported.
A radiant and convective heat flux sensor and a radiant heat flux sensor were placed on the panel's surface. Both sensors were built by *CAPTEC Enterprise*.
Fluid temperatures were sensed using Pt1000, see Figure **??**, which are resistance temperature detectors with a platinum thread. These sensing tools are placed inside the pipes, and were located at the inlet and outlet of the radiant panel, at the inlet and outlet of the chiller, and at the inlet and outlet of the water tank.
Fluid pressure was sensed at the inlet and outlet of the radiant panel with an *Omega PX139 Differential Pressure Sensor*, and in the water tank with pressure transducers, although the pressure changes turned out to be negligible and safe for all purposes intended during experimentation, see Figure **??**.
Also fluid mass rate was measured with a *Signet Scientific MK508 Flowmeter* located at the inlet of the radiant panel, see Figure **??**.
Location of the sensors are represented in Figure **??**.

2.6 Data Recollection

The *Agilent 34970A Data Logger* reaches a computer by *RS-232* and pours the data to a small application, where the calibration curves for each sensor have been programmed to interpret data into physically meaningful values. The application's creation process with *HPVEE* software is described in Appendix **??**. These values are simultaneously saved into a *comma-separated value* archive.

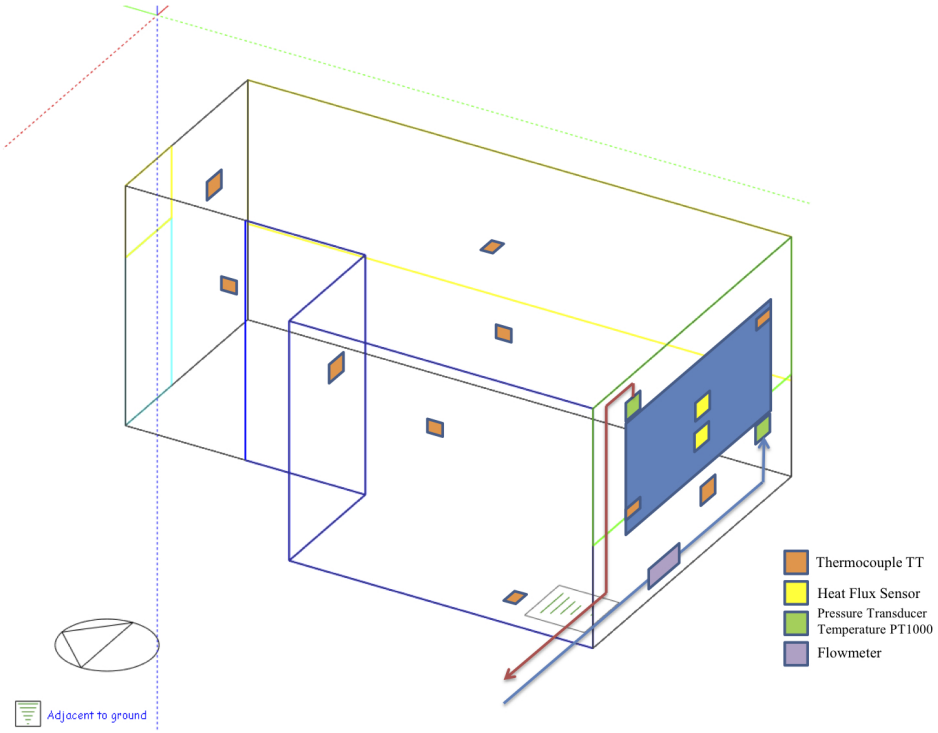

Figure 2.5: Sensors placement inside the *Test Room*. The panel was installed with surface thermocouples (orange) and heat flux sensors (yellow). In the pipes a flowmeter (purple) and thermoresistances (green) monitor water's flux. All surface temperatures in the room, including the panel, are captured using thermocouples (orange).

Chapter 3

Computer Modeling

A virtual model of the *test room* was first created using the graphical interface *DesignBuilder* and then simulated with the software *EnergyPlus*. In these two packages the geometry, envelope materials, thermal loads, and conditioning systems can be reproduced in detail; constant development in the heat transference algorithms and material properties are turning *EnergyPlus* in the standard tool for building evaluation.

3.1 Climatic Archive

Two working climatic stations are set in the tallest buildings of the IER. They gather data of direct solar radiation, diffuse solar radiation, global solar radiation, dry bulb temperature, wet bulb temperature, relative humidity, wind speed, wind direction, and barometric pressure. The data is averaged and recorded in ten-minute intervals throughout the year. A special format of this information is fed to the software simulator in order to create accurate site conditions. By using climatic information in situ, the most accurate weather simulation is achieved and, in consequence, the most faithful thermal simulation of the *test room* is resolved. All the data collected by the weather stations form a very complete batch, quite adequate for the purposes intended in this section of the study.
EnergyPlus has an auxiliary program that creates a weather data file with the *.epw* format, used during the simulation. In Appendix **??**, the process to create this file can be consulted.

3.2 DesignBuilder Model

DesignBuilder is a graphic modeling environment where virtual buildings performance can be tested [**?**]. Model Construction becomes easier having a visual representation of the geometry of the building. Also, important thermal characteristics can be assigned: site altitude, global location, and weather; material properties such as density, heat capacity, and absorptivity are specified to every envelope surface and partition, as well as glazings and openings; room thermal loads of equipment, lightning, use and occupancy; HVAC systems, natural and mechanical ventilation, domestic hot water, and even infiltration; schedules for each variable according to building usage can also be programmed; heat transfer constants; and standard or local certification criteria to evaluate the building's performance. *DesignBuilder* includes a large and reliable library of properties described in every field, nevertheless, they can be customized.

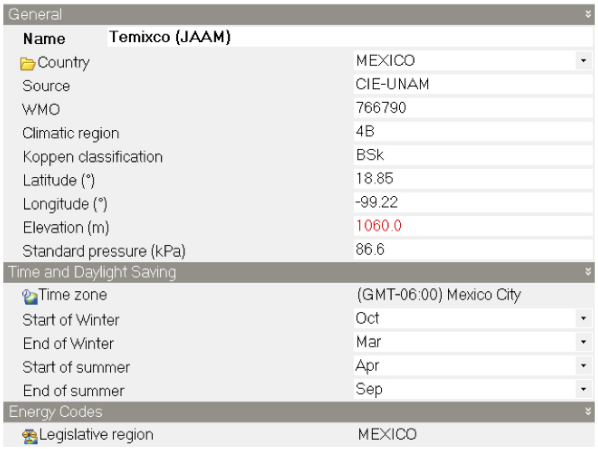

Figure 3.1: Location Template. Site climatic characteristics are set.

3.2.1 Creating the Model

In this section, the input windows that describe the model in *DesignBuilder* will be described. Also, the specific data for this particular model is presented.

Location

Location data uses the climatic archive referred above which, with enough information available, creates an statistic and geo-positioning archive. This archive will be read by the software to fill the following information, see Figure **??**:

- WMO (World Meteorological Organization) number, which is a classification for the international exchange of information related to meteorology. Temixco belongs to the station number *766790* [**?**], which corresponds to Mexico City's Benito Juárez International Airport [**?**]. In spite of the proximity of the weather station, elevation changes drastically and so does the weather; this and the logical advantages of having local weather data, called the decision to use our own customized climatic archive.

- Climatic region according to ANSI/ASHRAE standard 169-2006 [**?**]. Classification 4B is defined as dry weather with no direct marine contact, where precipitations are between 2500 and 3000 mm.

- Latitude: 18.85°; longitude: $-99.22°$; and elevation:1280 $m.a.s.l.$

- Standard Pressure: 86.6 kPa.

- Time zone and season intervals for daylight saving, set to GMT-06:00.

- Legislative region for energy codes: some countries grant buildings special classification according to their use and energy consumption.

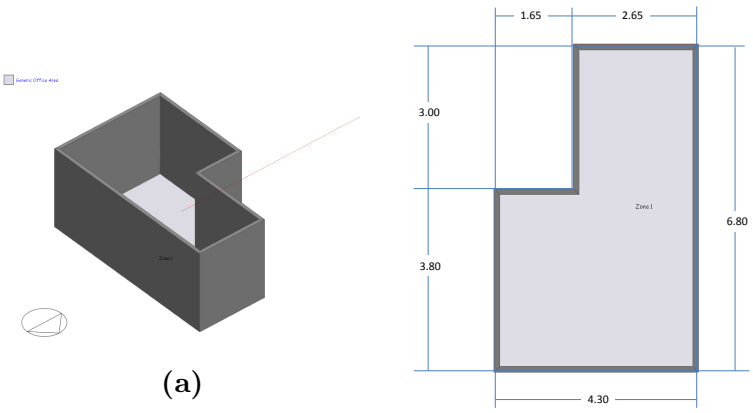

(a) (b)

Figure 3.2: L-shaped computer room. North-east view and ground view.

- Winter and summer design weather: these are the hottest and coldest weeks of the year, which are used as the extreme conditions in at which the model would be exposed.
- Hourly weather data for simulations.

Building Geometry

Using dimensions measured in the *test room*, these next steps were followed to create the model. In Figure **??** a visual representation of each step can be seen.

1. The envelope's plan is traced on the drawing space. The height extrusion of the model is set to 3.00 m. Inner partitions, which delimit the *Test Room* are also traced. Care was taken in order to achieve the correct orientation, although it can be corrected afterwards, see Figure **??**.

2. The rest of the inner partitions are drawn, creating several thermal zones. Automatically, each zone is named *"Zone n"*. In this case, the *test room* is called *CC*, which stands for Computer Center. See Figure **??**.

3. Windows and doors are marked in every surface of the envelope or the partitions. *Zone CC* has a northern door under a non-operable window and a large eastern window, operable 40%, see Fig.**??** and Figure **??**.

4. After the envelope has been extruded and its openings declared, solar protection and the adjacent two-story building located in the southern face are traced. These parts are described using *DesognBuilder*'s component blocks, denoted in purple. This kind of blocks have no thermal mass, but shadows are still casted over the adjacent buildings; in this manner, negligible calculation accuracy is sacrificed and lighter

simulation processes are accomplished. The outer hall is limited and half-buried with soil blocks, depicted in green, see Figure **??**.

5. In the early hours, significant solar radiation would reach the east openings if a set of offices and plants weren't protecting the facade. The offices where modeled, again with component blocks that cast shadow upon the laboratory building, see Figure **??**.

6. An alternative to represent the shadows casted by the adjacent offices and plants is to place a fake wall, constructed with component blocks, in front of the hall. Different transmissivity coefficients can be tested to resemble reality or simulate different conditions, see Figure **??**.

Once the building geometry has been modeled, the thermal properties and charges are set in the model.

Activity

The activity section lets the usage of the building be defined. In the *test room*, typical office activities are held, mostly in office hours. All the activities in this tab have been scheduled from 8:00 to 18:00 hours, Monday through Saturday, see Figure **??**. The particular characteristics are set to:

- Occupation in the room is usually between 0 to 6 people. Occupancy density of 0.250 $people/m^2$ is entered, which corresponds to 6 people, the less favorable scenario.

- As mentioned before, simple office activities are held in this part of the laboratory, so a low metabolic rate, such as *typing* is specified in this denomination (approximately 1.1 MET).

- 0.5 to 1.0 CLO corresponds to typical light informal clothing. Shorts and a t-shirt during summer; pants and shirt during winter [**?**].

- Other important thermal load in an office space is the equipment. According to the typical heat gains referred before, in section **??**, 22 W/m^2 correspond to computers and laptops, and 4 W/m^2 to other office equipment; printers, scanners and such.

Construction

Each construction material can be assigned with physical properties of their own, either taken from *DesignBuilder*'s libraries or user entered. Geometric (thickness, dimensions) and composition (layers) values were measured in the *test room*. This model uses thermal and optical properties that have been used for previous investigations at IER [**?**, **?**]. Constructing materials are assigned as follows:

- *External walls.* Red brick walls of 0.120 mm thickness.

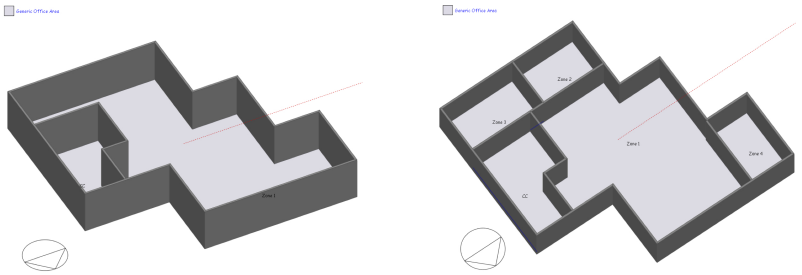

(a) Envelope geometry.

(b) Internal partitions.

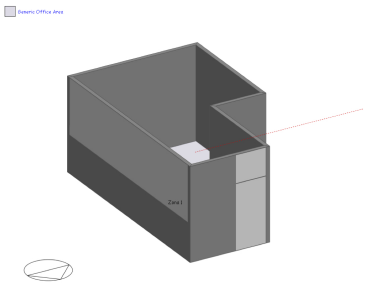

(c) External openings in *test room*.

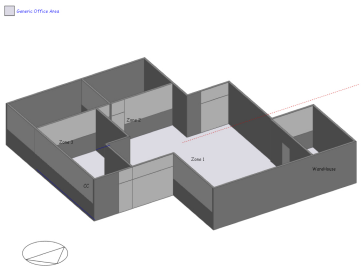

(d) Internal openings.

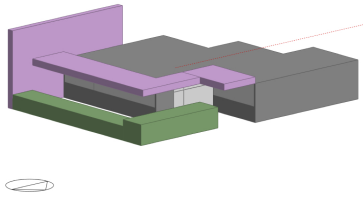

(e) Solar protection eaves.

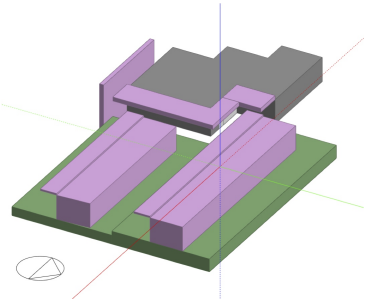

(f) Adjacent buildings.

Figure 3.3: Building modeling procedure.

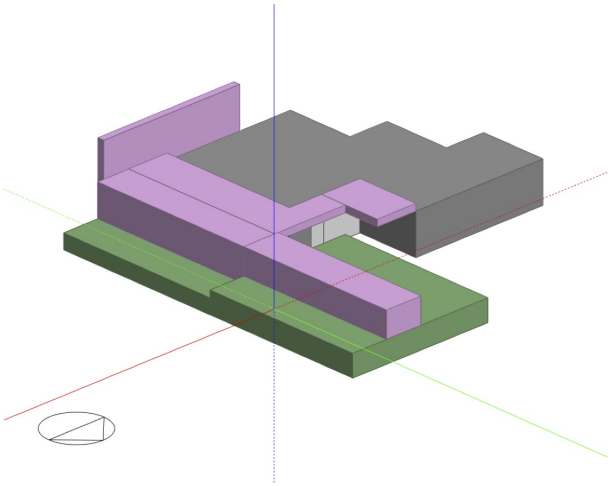

Figure 3.4: Laboratory virtual model with fake wall, equivalent to adjacent buildings and greenery.

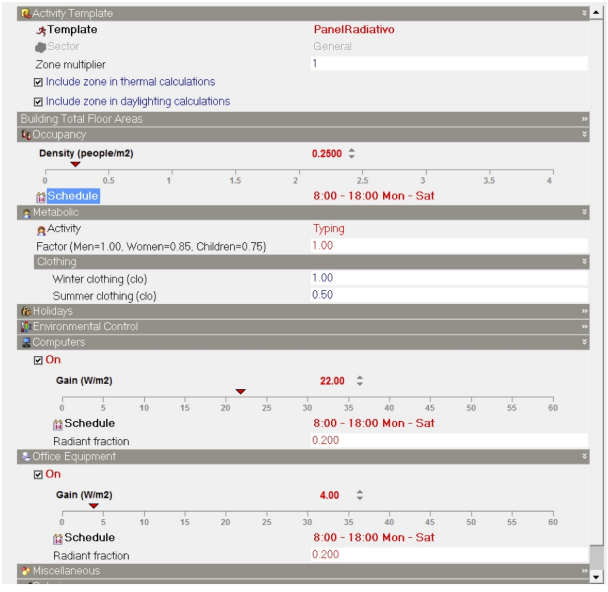

Figure 3.5: Activity Tab. Office schedule is set for occupation and equipment.

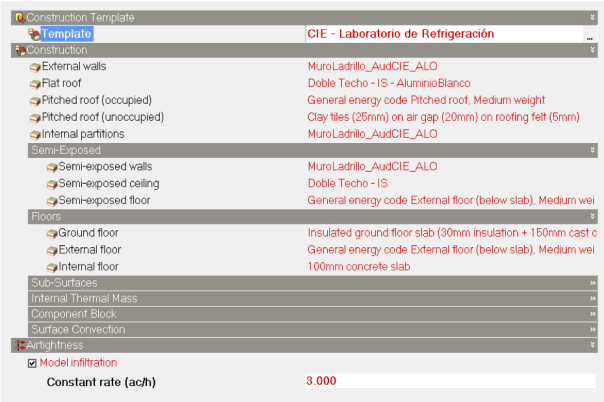

Figure 3.6: Construction Tab. Materials' characteristics are assigned to each buiilding surface.

- *Flat Roof.* Composite roof made of 6 layers: asphalt, mortar, expanded polystyrene, high density concrete, aerated concrete, and an aluminum plate painted white. The last aluminum layer will cover the tubing of the simulated radiant panel. See Figure **??**.

- *Semi-exposed walls.* Constructed with red brick walls of 0.120 *mm* thickness, as well. The semi-exposed walls correspond to areas that are not totally closed, such as the hall that surrounds the *test room*.

- *Semi-exposed ceilings.* Built with a similar composition of the *Flat roof*, except for the inmost aluminum layer, which is obviated since no tubing is placed in semi-exposed ceilings. They also correspond to the hall outside the *test room*, which is not fully closed.

- *Internal floor.* Concrete slab of 0.100 *mm* thickness.

- *Wall sub-surfaces.* Drywall in part of the west side of the *test room*.

- *Airtightness.* Constant rate of 0.50 *ACH* (Air Changes per Hour, i.e. the rate in which the volume of air in the room is renewed in an hour, in this case with natural ventilation); input is a typical value for natural ventilation xxx.

- *Other components.* The rest of the constructive components have little relationship in the thermal behavior of the *test room*, hence default properties were kept.

Table **??** lists the physical properties for each component.

Glazing

Simple glazing is used in the whole laboratory. The laboratory, including the *test room*, has single 0.006 *mm* clear glass panes, aluminum dividers, and 40% area operability. These values are set for external windows. Internal windows are the same except in the *test room*, where no-glazing windows is the case, see Figure **??**.

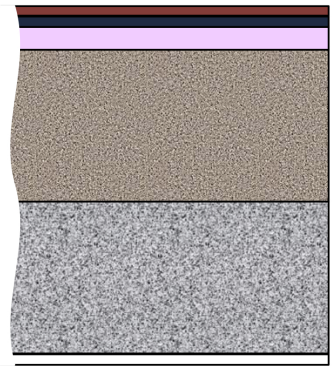

Figure 3.7: Flat roof. From top to bottom: 0.015 m of asphalt, 0.010 m of mortar, 0.020 m of expanded polystyrene, 0.200 m of high density concrete, 0.200 m of aerated concrete, and aluminum plate of 0.003 m. Not to scale.

Construction Materials Properties								
	Constructed in	Thickness (m)	Conductivity (W/mK)	Specific heat (J/kgK)	Density (kg/m3)	Thermal absorptance	Solar absorptance	Visible absorptance
Brick Wall	External walls, internal partitions, semi-exposed	0.12	0.95	1070	1800	0.9	0.6	0.6
Asphalt	Flat roof	0.015	0.7	920	2100	0.9	0.7	0.7
Mortar*	Flat roof	0.01	0.88	896	2800	0.9	0.6	0.6
XPS*	Flat roof	0.02	0.04	1400	15	0.9	0.7	0.7
HD Concrete*	Flat roof	0.2	2	1000	2400	0.9	0.6	0.6
Aerated	Flat roof	0.2	0.16	840	500	0.9	0.6	0.6
Aluminum,	Flat roof in Test Room	0.003	160	880	2800	0.3	0.9	0.9
Gypsum	Internal sub-surfaces	0.025	0.25	1000	900	0.9	0.5	0.5
Air Gap*	Internal sub-surfaces	0.1	0.3	1000	1000	0.9	0.7	0.7
Concrete Slab	Internal floor, semi-	0.1	1.4	840	2100	0.9	0.6	0.6

Table 3.1: Physical and optical properties for envelope and internal partitions constructing materials. Materials marked with star (*) are internal layers of a construction system, hence optical properties are irrelevant. These properties are taken from DesignBuilder's library of materials, except for thickness, which are the real values in the building.

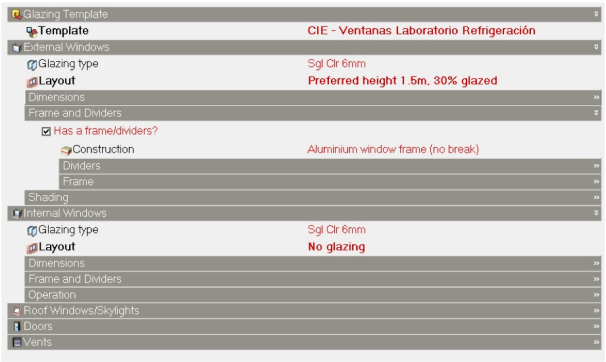

Figure 3.8: Openings Tab. Windows, frames, and dividers characteristics.

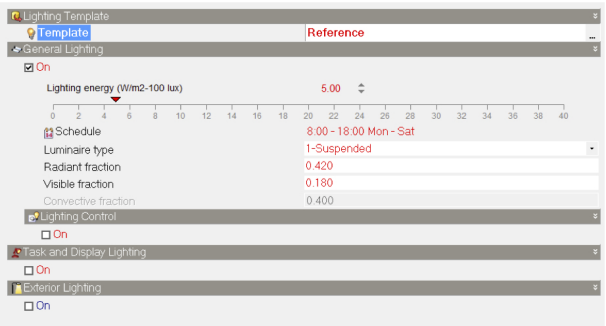

Figure 3.9: Lighting Tab. Schedule, control, and energy consumption used in general lighting.

Lighting

The *test room* has two energy-saving lamps, hanging, no luminaries. According to the recommended thermal loads in Table **??**, the lightning energy is set to 5.00 W/m^2 – 100 lux. Lighting also has an office schedule from monday to saturday, 8:00 to 18:00 hrs, see Figure **??**.

Ventilation

No vents or mechanical ventilation systems are installed in the *test room*. Only natural ventilation is present in small velocities; it is set to 0.500 ACH and a programmed schedule on, since windows are rarely closed, see Figure **??**.

3.2.2 Chilled Envelope System

DesignBuilder allows the creation of a radiant surface by first assigning a location between two surfaces for tubing, then generating a system to feed the tubing, and finally providing operation conditions (tubing geometric constrains, operating temperatures, schedule, operation control).
The *flat roof* covering the *test room* has been assigned with an inner source between the

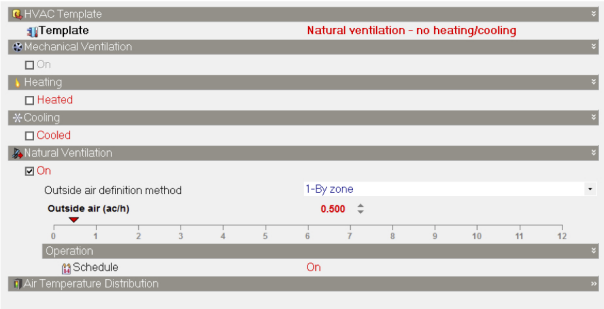

Figure 3.10: HVAC Tab. No mechanical systems used, only natural ventilation.

last two layers, which means that between the aerated concrete and the aluminum plates is a space for internal tubing. The latter layer was modeled considering two reasons: commercial chilled water systems have a metallic plate as exposed view to the users so in this way it would resemble such systems, and furthermore, it allows us to model a internal source closer to the surface, since *DesignBuilder* needs for it to be in-between two layers. Also, the emissivity factor (α) was modified to $\alpha = 0.9$ which is the value present in real conditions.
The simplest way to create a chilled water system that will feed the radiant tubing surface is to generate a chilled water loop (CHW Loop in Figure **??**). Then, connecting it to the surfaces in which the internal source has been created; the *test room* ceiling in this case. The chiller in the chilled water loop needs a cold fluid source; for this purpose a condenser loop (condenser loop supply side and condenser loop demand side in Figure **??**) is connected. The water delivered to the radiant system tubing is set to 15°C; this is the only variable controlled in the loops, since these systems escape the span of the study. Every other variable is set as default.
Once the working fluid loop has been made, the chilled surface can be designed. The following settings are introduced, see Figure **??**:

- *Tubing settings.* The tubes have an inner diameter of 0.005 m and a total length of 360.0 m distributed through all the surface.
- *Flow rate.* Fixed on 0.00075 m^3/s, that correspond to the value measured during experimentation.
- *Pump flow rate schedule.* Always on.
- *Condensation type control.* Always off. In real operation conditions the panel worked continously, and no condensation control was implemented.

Every one of the aspects in the *DesignBuilder* model approaches the research to a better reproduction of the experiment. Although *DesignBuilder* can also simulate the operation process, some simplifications in weather conditions were observed, which result in a reasonable first approximation, but not always accurate enough. In consequence, the program *EnergyPlus* was run to accomplish better results.

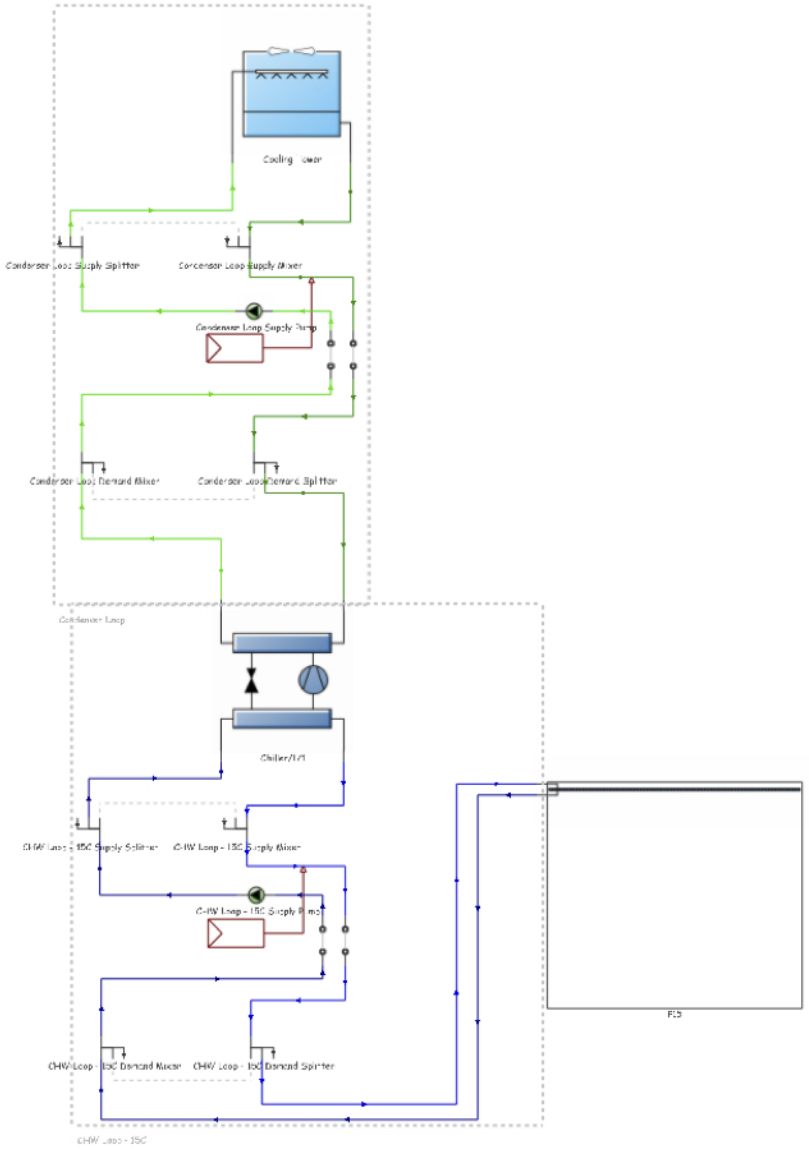

Figure 3.11: Radiant panel system. The loop includes condenser that supplies refrigerating fluid to the condenser; the chilled water loop, which delivers water at the set temperature; and the radiant panel located in the *test room*.

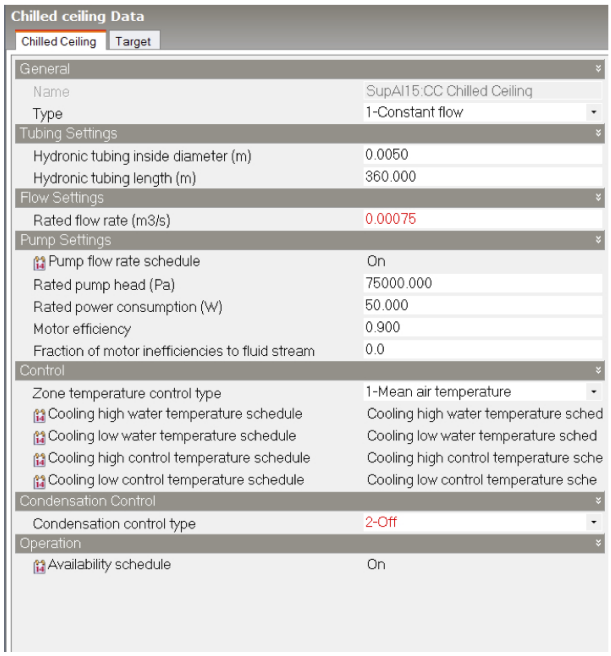

Figure 3.12: Radiant panel's geometric values, power and control settings.

3.3 EnergyPlus Model

EnergyPlus is a tool designed to analyze buildings with all their associated thermal loads [**?**]. Although it is a stand-alone simulation engine, files can be imported from modeling programs, such as *DesignBuilder*. This way, information input becomes easier and more efficient.
DesignBuilder can export an IDF file that can be read by *EnergyPlus*. The IDF file includes the construction geometry and materials, as well as the usage captured in the *DesignBuilder* environment. Albeit, it can be all modified through the *IDF Editor* of *EnergyPlus*.
After the file is exported, a simulation can be run using the same pre-existing weather file, and *EnergyPlus* will throw out a large collection of results from which it will be to our interest to analyze room and surface temperatures regarding the *test room*.
Simulation results include: heat balance solutions, transient heat conduction, mass transfer, fenestration calculation, daylight and HVAC controls, and even atmospheric pollution calculations [**?**]. In our case, the key result out of this wide group is the simulated radiant temperature. The results are written in a tab-separated file that contains the value of each variable in the assigned time-step.
The *definition* file written for this study throws out the following results for the *test room*:

- *Room Radiant Temperature.* Essential variable to evaluate the radiant panel's performance.

DesignBuilder Model Summary				
	Class	Subclass	Quantity	Unit
Activity	Occupancy	People density	0.25	people/m2
	Metabolic	Typing	1	MET
	Clothing	Clothing summer	0.5	CLO
		Clothing winter	1	CLO
	Gains	Computer	22	W/m2
		Office equipment	4	W/m2
Openings	Glazing type	Single clear 6mm	-	-
	Frame and dividers	Aluminum	-	-
	Internal windows	Single clear 6mm, No glazing	-	-
Lighting	General	Energy	5	W/m2-100lux
HVAC	Natural ventilation	Outside air	0.5	ac/h

Table 3.2: Input data entered in *DesignBuilder*. These values were taken from the *test room* except for the ventilation, which was matched to a typical value.

- *Room Dry Bulb Temperature.* Useful to validate simulations against experimentation.
- *Inside Surface Temperature.* Radiant calculations stated in ASHRAE Fundamentals Handbook require planar surface temperatures [**?**].
- *Radiant Panel Heat Transference.* Variable measured during experimentation that also validates and evaluates the radiant panel's performance.

Once the model is fully defined through the IDF file, the remaining action before the analysis is to click the simulation button. A ten-minute interval was set as time-step and simulated for 24 hours in the same days when experimental data was captured.

3.4 Modeling Summary

Table **??** summarizes the data entered to the virtual model that describes the occupancy, envelope and partition characteristics, equipment use, and schedules, as well as the radiant panels design properties.

Chapter 4

Analysis

4.1 Experimental Results

The radiant panel was experimentally evaluated during four days in 24-hour tests, from 00:00 to 23:59 hrs through regular office working conditions: low people occupancy, office equipment on, low lighting, natural ventilation (air velocity $v_{ar} \approx 0.1\ m/s$). Data was retrieved in ten-minute intervals. Results for four days are here presented.

Day 1

Water flow rate averaged at $\overline{F}_{w,in} = 72.7 \times 10^{-6}\ m^3/s$ ($\sigma = 0.01$) in the inlet of the radiant panel. The mean temperature of the fluid at the entrance of the panel was of $\bar{t}_{w,in} = 13.7\ ^{\circ}C$ ($\sigma = 0.57$) and at the exit the temperature raised $\Delta_t = 0.63\ ^{\circ}C$; while mean radiant heat flux into the panel resulted in $\overline{q}_{rad} = 26.5\ W/m^2$ ($\sigma = 1.22$).

Day 2

During the second test, the panel absorbed $\overline{q}_{rad} = 30.0\ W/m^2$ ($\sigma = 3.30$) when chilled water flowed at $\overline{F}_{w,in} = 72.5 \times 10^{-6}\ m^3/s$ ($\sigma = 0.02$) with an incoming temperature of $\bar{t}_{w,in} = 13.4\ ^{\circ}C$ ($\sigma = 0.87$). At the outlet, the water temperature increased by a $\Delta_t = 0.50\ ^{\circ}C$.

Day 3

The water temperature at the inlet was $\bar{t}_{w,in} = 13.6\ ^{\circ}C$ ($\sigma = 0.54$) and was raised by an average of $\Delta_t = 0.64\ ^{\circ}C$ during the third day. The radiant heat flux during the test reached $\overline{q}_{rad} = 31.0\ W/m^2$ ($\sigma = 0.68$) with a water flux rate of $\overline{F}_{w,in} = 64.8 \times 10^{-6}\ m^3/s$ ($\sigma = 0.83$).

Day 4

Chilled water flowed into the panel with an average temperature of $\bar{t}_{w,in} = 13.8\ ^{\circ}C$ ($\sigma = 0.49$) and average volumetric flow rate of $\overline{F}_{w,in} = 25.5 \times 10^{-6}\ m^3/s$ ($\sigma = 0.87$). The radiant panel gained and average radiant heat flux of $\overline{q}_{rad} = 30.8\ W/m^2$ ($\sigma = 0.75$), increasing the water's temperature by a delta $\Delta_t = 0.40\ ^{\circ}C$ at the outlet.
Figures **??** through **??** display radiant and outdoors temperature for each day; with a purple line, radiant temperature, and the outdoors temperature with a green dotted line.

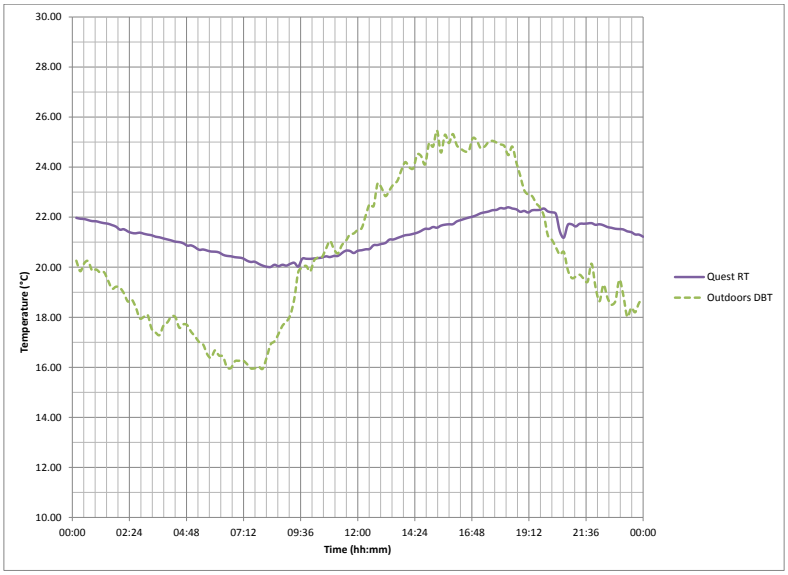

Figure 4.1: Day 1. Radiant temperature (purple line) outdoor dry bulb temperature (green dotted line) as function of time.

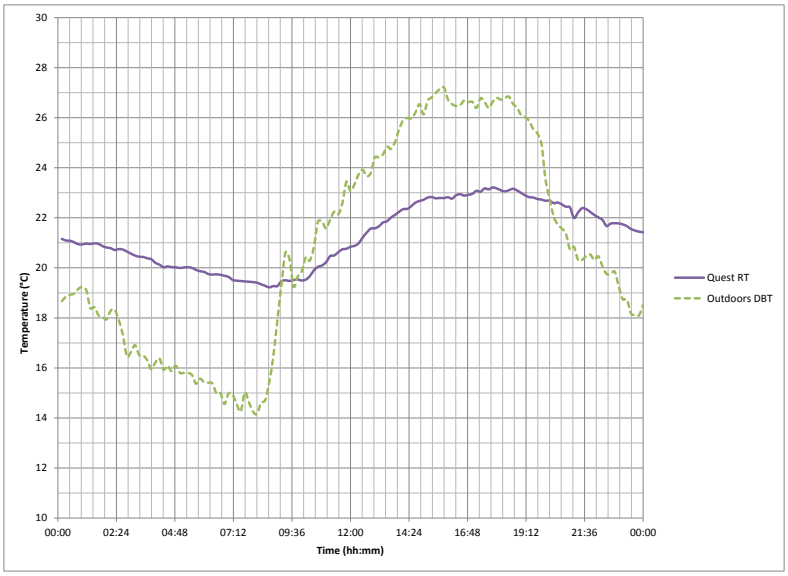

Figure 4.2: Day 2. Radiant temperature (purple line) outdoor dry bulb temperature (green dotted line) as function of time.

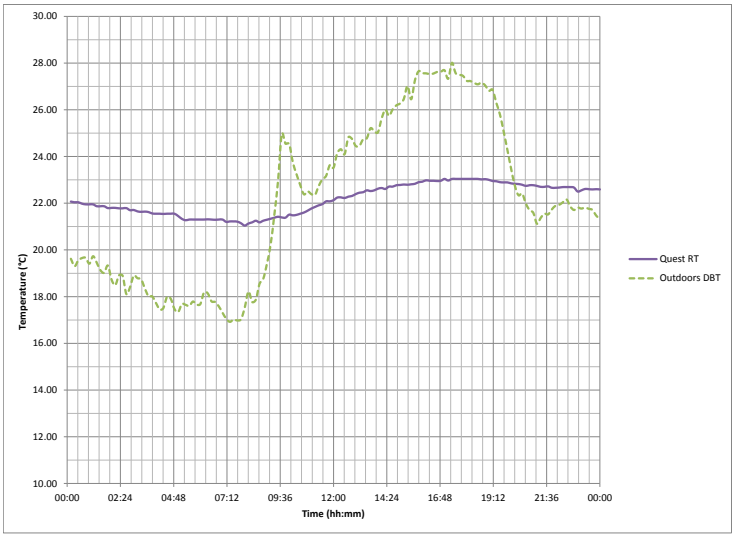

Figure 4.3: Day 3. Radiant temperature (purple line) outdoor dry bulb temperature (green dotted line) as function of time..

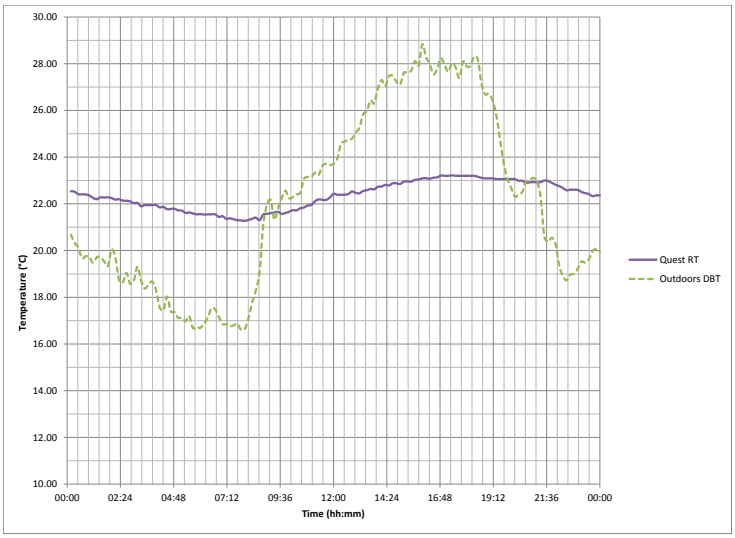

Figure 4.4: Day 4. Radiant temperature (purple line) outdoor dry bulb temperature (green dotted line) as function of time.

There exists a difference between the temperatures of the water flowing inside the panel and the surface of the radiant panel of approximately 1 $°C$; the temperature at the surface is the one at which the inside of the room *sees* the panel.

4.2 EnergyPlus Results

The chilled water system was fixed to have a flow rate of $F_{w,in} = 75 \times 10^{-6}\ m^3/s$ and a water temperature of $t_{w,in} = 15\ °C$ at the inlet. Under these conditions, *EnergyPlus* delivered the following results.

Day 1

During test day one the radiant temperature average of $\bar{t}_r = 20.15\ °C$ ($\sigma = 1.04$) and an increase of $\Delta_t = 0.47\ °C$ in the water temperature. The panel transferred a average flux of $\overline{q}_{rad} = 32.1\ W/m^2$ ($\sigma = 8.37$).

Day 2

The second test day simulation resolved a heat transference to the panel of $\overline{q}_{rad} = 33.8\ W/m^2$ ($\sigma = 0.54$) ($\sigma = 10.97$), and the room had a radiant temperature average of $\bar{t}_r = 20.39\ °C$ ($\sigma = 1.52$). Water temperature was raised by $\Delta_t = 0.49\ °C$ when it exited the panel.

Day 3

In the third day simulation, an average radiant temperature was of $\bar{t}_r = 21.10\ °C$ ($\sigma = 1.40$) with a water temperature difference of $\Delta_t = 0.55\ °C$. The radiant panel absorbed $\overline{q}_{rad} = 38.1\ W/m^2$ ($\sigma = 10.66$).

Day 4

The last simulated day resolved an average radiant temperature was $\bar{t}_r = 21.32\ °C$ ($\sigma = 1.40$), while $\overline{q}_{rad} = 39.2\ W/m^2$ ($\sigma = 10.61$)were absorbed. The water temperature difference between inlet and outlet averaged at $\Delta_t = 0.58\ °C$.

Figures **??** through **??** display radiant temperatures and outdoors temperature for each day; with a purple line, *QUESTemp* radiant temperature, a blue line for EnergyPlus radiant temperature, and the outdoors temperature with a green dotted line.
In Table **??** temperatures, heat flux, and flow mass rate are reported for both experimental and simulated results.

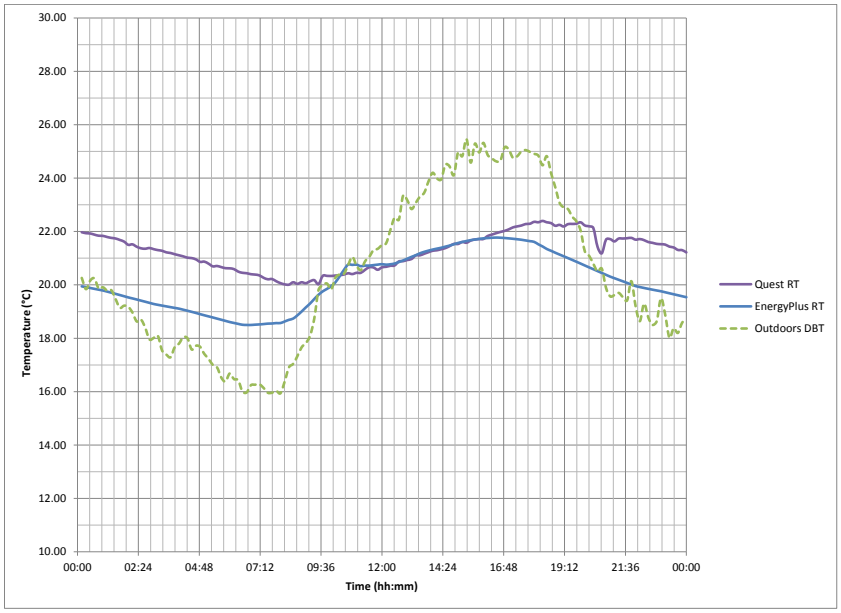

Figure 4.5: Day 1. Radiant temperature comparative: QUESTemp measured and simulated using EnergyPlus.

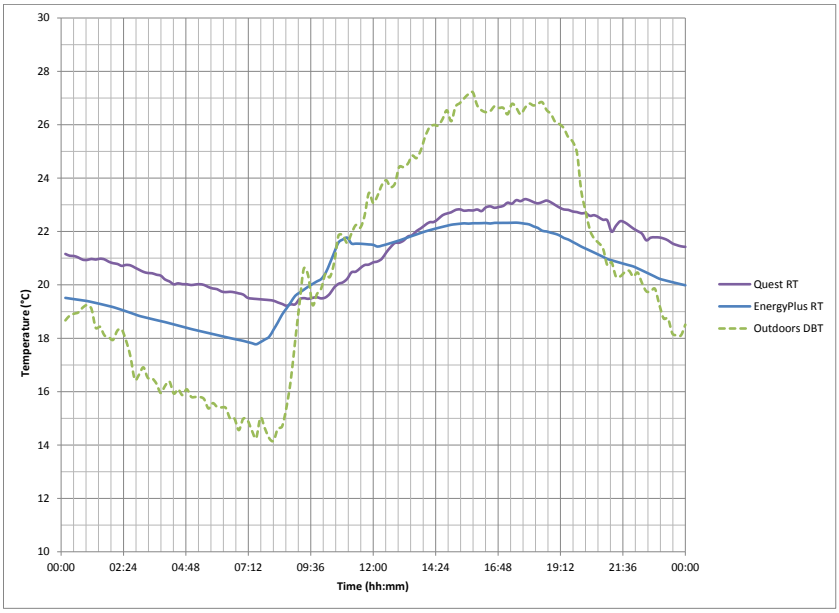

Figure 4.6: Day 2. Radiant temperature comparative: QUESTemp measured and simulated using EnergyPlus.

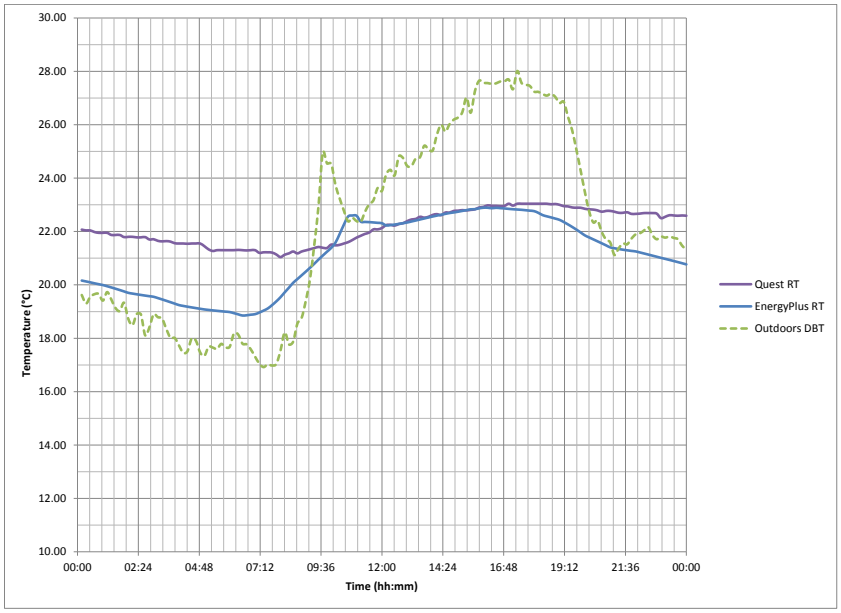

Figure 4.7: Day 3. Radiant temperature comparative: QUESTemp measured and simulated using EnergyPlus.

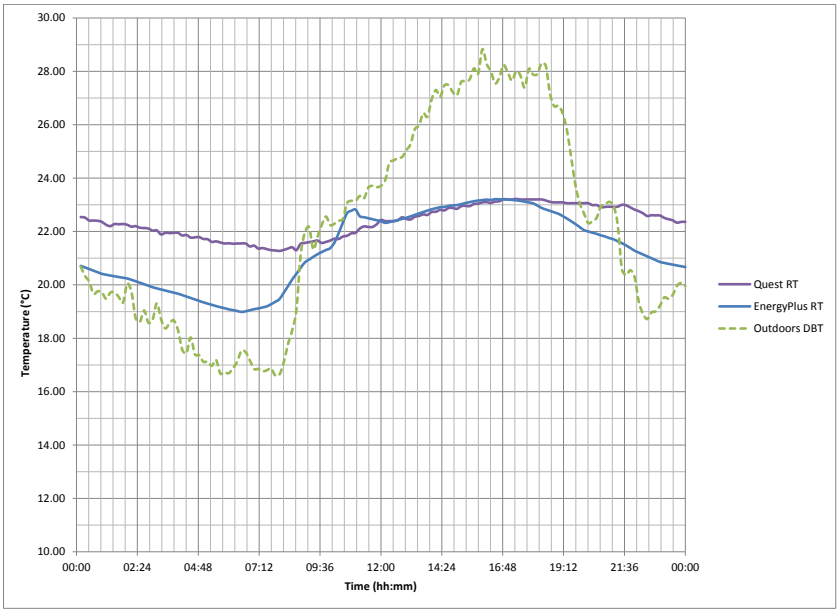

Figure 4.8: Day 4. Radiant temperature comparative: QUESTemp measured and simulated using EnergyPlus.

		Experimental				Simulated			
	Test Day	**Day 1**	**Day 2**	**Day 3**	**Day 4**	**Day 1**	**Day 2**	**Day 3**	**Day 4**
Mass Flow Rate (m^3/s)	Average	72.7E-06	72.5E-06	64.8E-06	25.5E-06	75.0E-06	75.0E-06	75.0E-06	75.0E-06
	Maximum	73.4E-06	73.4E-06	73.3E-06	36.6E-06				
	Minimum	72.1E-06	71.6E-06	35.1E-06	23.0E-06				
Temperature at the Inlet (°C)	Average	13.7	13.4	13.6	13.8	15	15	15	15
	Maximum	15.4	14.7	14.3	14.5				
	Minimum	12.9	12.2	12.8	13.0				
Temperature at the Outlet (°C)	Average	14.3	13.9	14.2	14.3	15.5	15.5	15.6	15.6
	Maximum	16.1	15.2	14.9	15.0	15.7	15.8	15.9	15.9
	Minimum	13.5	12.7	13.5	13.5	15.3	15.3	15.4	15.4
Temperature Difference (°C)	Average	0.63	0.50	0.63	0.53	0.47	0.49	0.55	0.58
	Maximum	0.68	0.66	0.70	0.56	0.70	0.80	0.87	0.89
	Minimum	0.53	0.42	0.55	0.48	0.30	0.25	0.33	0.34
Panel Surface Temp (°C)	Average	15.1	14.9	15.0	15.3	15.5	15.5	15.6	15.6
	Maximum	16.4	16.5	15.8	16.1	15.8	15.9	16.0	16.0
	Minimum	14.2	13.5	14.1	14.3	15.3	15.3	15.4	15.4
Heat Flux (W/m^2)	Average	26.4	29.9	31.0	30.8	32.1	33.8	38.1	39.6
	Maximum	29.9	51.0	32.7	32.4	48.5	54.9	60.1	61.5
	Minimum	22.9	25.6	29.8	27.9	20.3	17.1	22.7	23.6
Radiant Temperature (°C)	Average	21.3	21.3	22.2	22.4	20.1	20.4	21.1	21.3
	Maximum	22.4	23.2	23.0	23.2	21.8	22.3	22.9	23.2
	Minimum	20.0	19.2	21.0	21.3	18.5	17.8	18.9	19.0

Table 4.1: Daily averages, maximums, and minimums for flow mass rate, inlet and outlet panel temperatures, panel surface temperature, radiant heat flux to the panel, and room's radiant temperature, for both experimental and simulated tests.

4.3 Data Comparison

The largest differences between measured radiant temperature and simulated radiant temperature appeared at 6 a.m., being of the order of 2.56 $^{\circ}C$. During working hours the differences were close to zero values. At mid-morning appears a peak in temperature simulations due to the direct solar radiation in the eastern facade. Figure **??** presents the radiant temperature differences for all four test days.

4.4 ASHRAE Radiant Temperature Calculations

Using the method described by ASHRAE Fundamentals Handbook, Equation **??** has been substituted with surface temperature values of each wall, using both experimental and simulated data [**?**]. North and west walls temperatures, which correspond to front and left directions, were assigned an equivalent temperature by averaging all the planar temperatures in each direction. Figures **??** trough **??** show the resulting radiant temperatures per day: QUESTemp measured temperature with purple, ASHRAE calculation using surface values taken from HPVEE experimental results measurements with a blue line, ASHRAE calculation using surface values taken from *EnergyPlus* simulation with a red line, and the outdoors dry bulb temperature with a green dotted line.

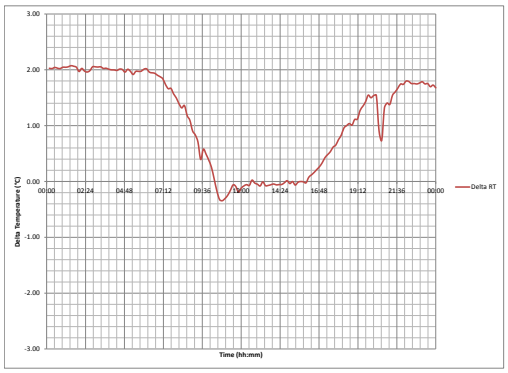

(a) Day 1.

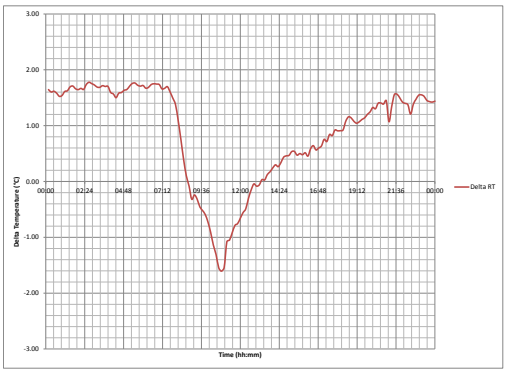

(b) Day 2.

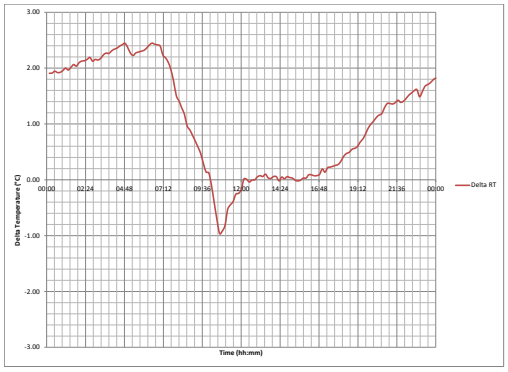

(c) Day 3.

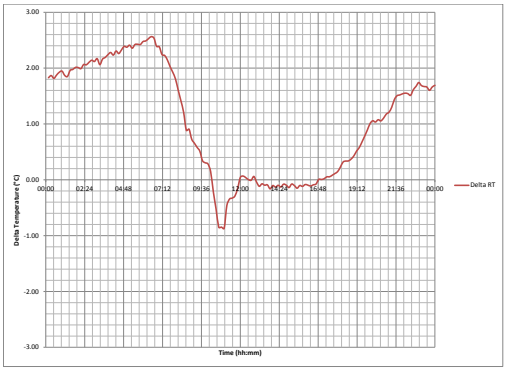

(d) Day 4.

Figure 4.9: Radiant Temperature differences between QUESTemp measured and EnergyPlus simulated values.

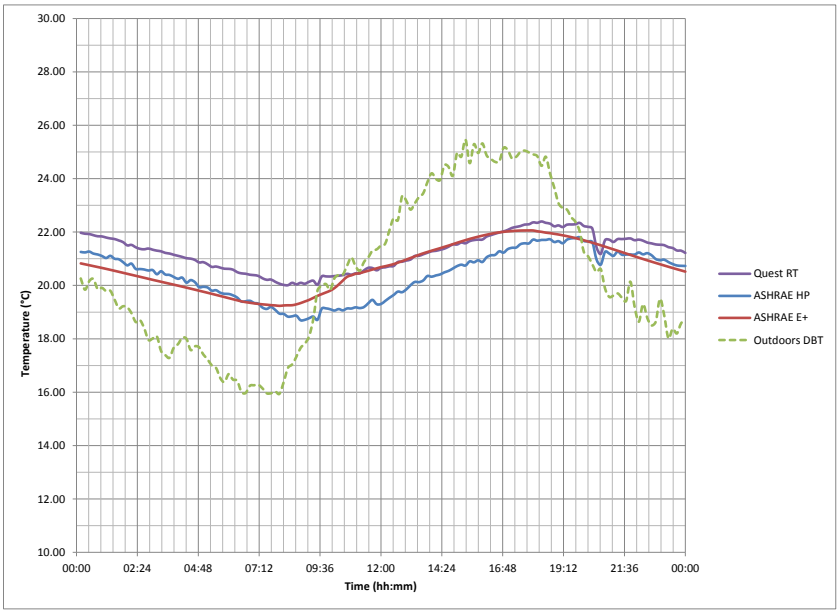

Figure 4.10: Day 1. Temperature as a function of time: the purple line represents the *QUESTemp* mean radiant temperature; the blue line represents the calculated mean radiant temperature using thermocouple readings and ASHRAE method, the red line graphs the mean radiant temperature calculated by EnergyPlus simulations and the ASHRAE method; the green dotted line is the outdoors dry bulb temperature as a reference of the day conditions.

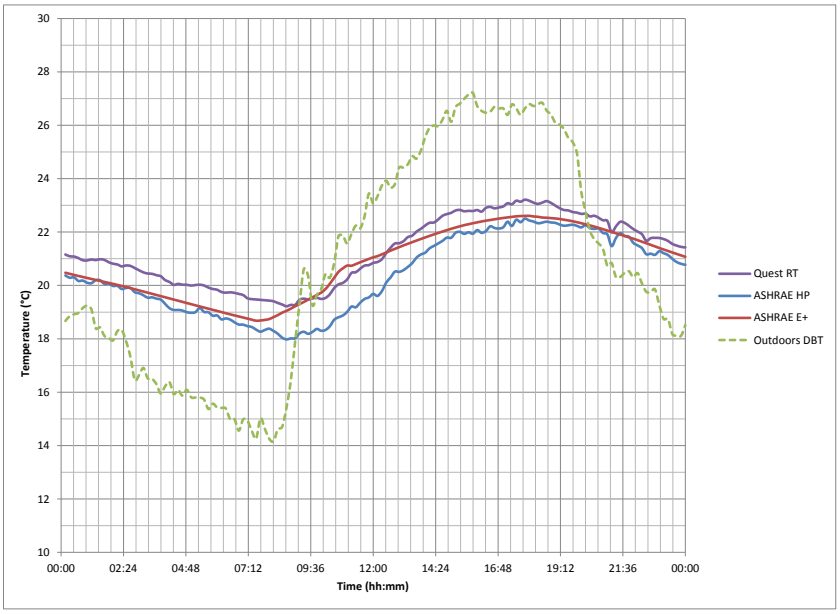

Figure 4.11: Day 2. Temperature as a function of time: the purple line represents the *QUESTemp* mean radiant temperature; the blue line represents the calculated mean radiant temperature using thermocouple readings and ASHRAE method, the red line graphs the mean radiant temperature calculated by EnergyPlus simulations and the ASHRAE method; the green dotted line is the outdoors dry bulb temperature as a reference of the day conditions.

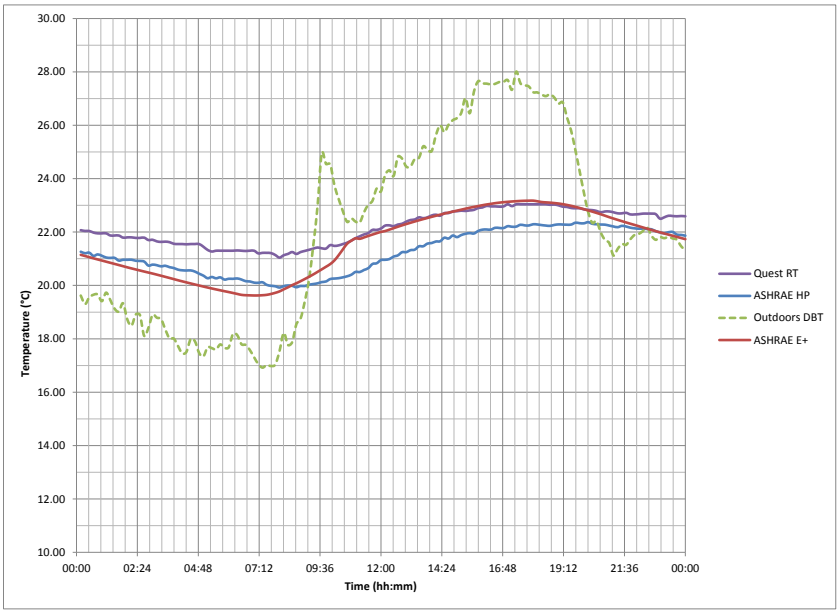

Figure 4.12: Day 3. Temperature as a function of time: the purple line represents the *QUESTemp* mean radiant temperature; the blue line represents the calculated mean radiant temperature using thermocouple readings and ASHRAE method, the red line graphs the mean radiant temperature calculated by EnergyPlus simulations and the ASHRAE method; the green dotted line is the outdoors dry bulb temperature as a reference of the day conditions.

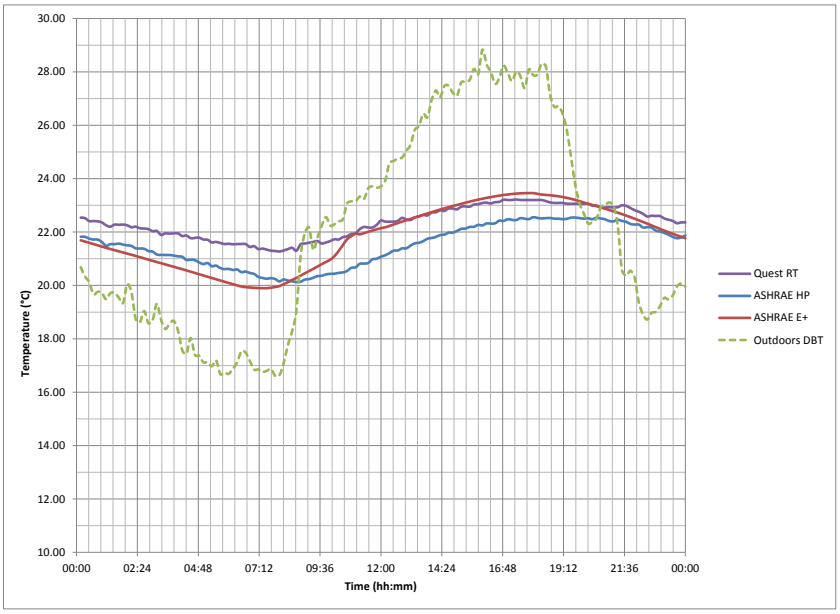

Figure 4.13: Day 4. Temperature as a function of time: the purple line represents the *QUESTemp* mean radiant temperature; the blue line represents the calculated mean radiant temperature using thermocouple readings and ASHRAE method, the red line graphs the mean radiant temperature calculated by EnergyPlus simulations and the ASHRAE method; the green dotted line is the outdoors dry bulb temperature as a reference of the day conditions.

Chapter 5

Results

A difference between experimental and simulated data is anticipated. QUESTemp has an accuracy of $\pm 0.5\ ^{\circ}C$. A propagation of bias error method was applied which resulted in a total error of $\pm 0.5\ ^{\circ}C$ for calculations that involve thermocouples type T measurements [**?**]. Additionally, ASHRAE Fundamentals Handbook gives this kind of thermocouples an uncertainty of $\pm 1.0\ ^{\circ}C$, and recommends the larger range. Simulated data that fall inside that range are to be considered accurate.

Beneath this criterion, *EnergyPlus* simulations give reliable information with a small amount of error. As it can be observed in Section **??**, when temperature starts to drop at nighttime, simulated data separates from experimental data and temperatures are under-calculated; whilst daytime values approximate fairly. During working hours, simulations offer a very good approximation; although during nighttime results become separated this can be explained because of xxx.

However, ASHRAE's mean radiant temperature calculation method using experimental surface temperatures in the room show that the radiant calculated temperature is less precise, but very close to measurements inside the acceptable ranges. It can be said that this calculation method describes the behavior of the temperature quite truthfully even it underestimates the values with little amount of error.

If radiant temperature is calculated with the ASHRAE method using surface temperatures obtained with *EnergyPlus* and from the experiments, an approximation equivalent to the same method using experimental surface temperatures is delivered. Table **??** shows the daily percentage of data inside the evaluation criteria.

In correspondence Table **??** shows the daily percentage of simulated data inside the $\pm 1.0\ ^{\circ}C$ ASHRAE's recommended range compared to the calculated radiant temperature using experimental surface temperatures.

		Simulated vs. Experimental			
	Test Day	Day 1	Day 2	Day 3	Day 4
Data In Range (±.5°C)	E+	32.6	19.4	35.4	36.8
	ASHRAE HP	5.5	8.3	4.2	5.6
	ASHRAE E+	45.1	52.8	50.0	56.2

		Simulated vs. Experimental			
	Test Day	Day 1	Day 2	Day 3	Day 4
Data In Range (±1.0°C)	E+	41.0	37.5	47.9	47.2
	ASHRAE HP	72.9	66.0	61.8	72.9
	ASHRAE E+	72.9	66.0	61.8	72.9

		Simulated vs. Experimental			
	Test Day	Day 1	Day 2	Day 3	Day 4
Data In Range (±1.5°C)	E+	53.5	62.5	59.7	80.0
	ASHRAE HP	100.0	100.0	100.0	100.0
	ASHRAE E+	100.0	100.0	100.0	100.0

Table 5.1: Percentage of data inside of range for the QUESTemp. Data in the range of $\pm 0.5\ ^{\circ}C$ is to be considered exact. A $\pm 1.0\ ^{\circ}C$ error is considered acceptable by ASHRAE standards.

		Simulated vs. Experimental			
	Test Day	Day 1	Day 2	Day 3	Day 4
Data In Range (±1.0°C)	E+	45.8	75.0	49.3	40.3
	ASHRAE E+	86.8	82.6	86.8	88.2

Table 5.2: Percentage of data inside recommended ASHRAE range of $\pm 1.0\ ^{\circ}C$ for thermocouple measurements.

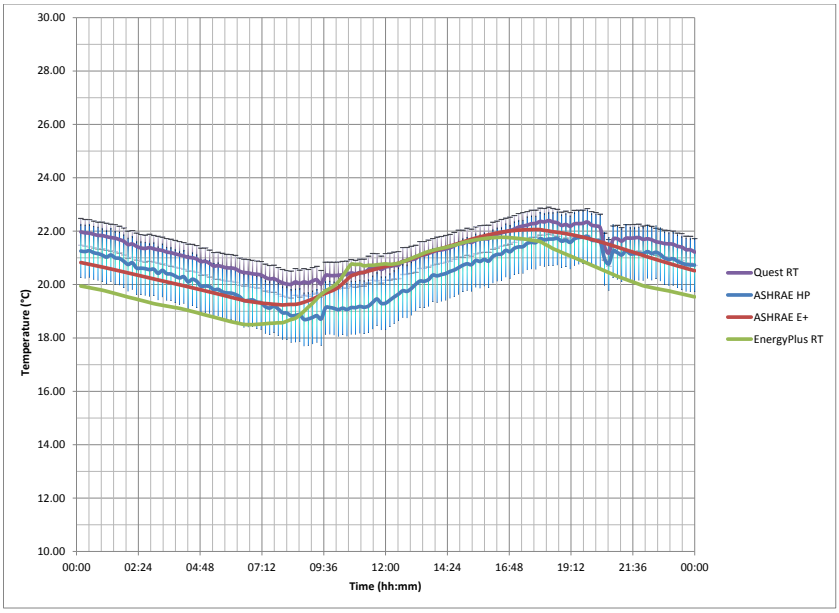

Figure 5.1: Day 1. The experimental values show in a shadow the range of error acceptable for each one: $\pm 0.5\ ^{\circ}C$ for *QUESTemp* (purple) and $\pm 1.0\ ^{\circ}C$ for ASHRAE method with thermocouples data (blue); the simulated mean radiant temperature using the ASHRAE method with *EnergyPlus* data (red) and the *EnergyPlus* simulated results.

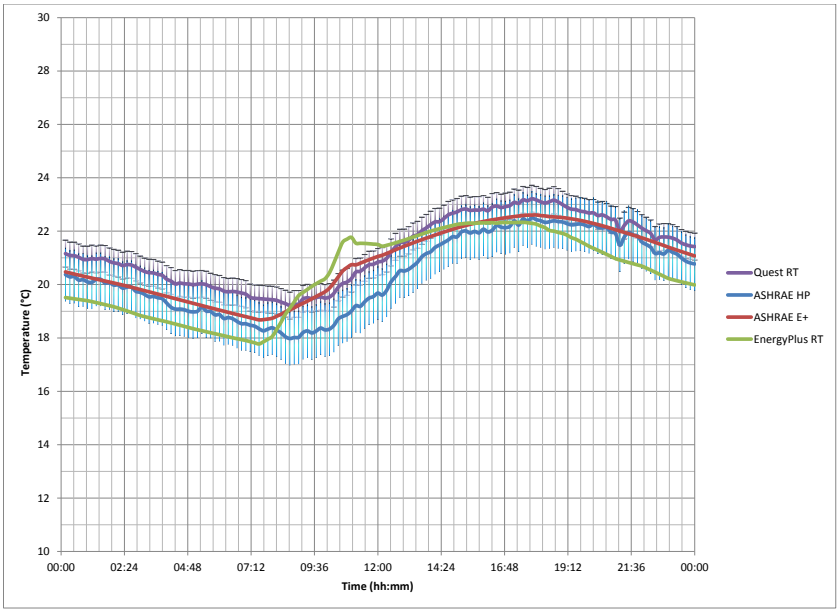

Figure 5.2: Day 2. The experimental values show in a shadow the range of error acceptable for each one: $\pm 0.5\ ^{\circ}C$ for *QUESTemp* (purple) and $\pm 1.0\ ^{\circ}C$ for ASHRAE method with thermocouples data (blue); the simulated mean radiant temperature using the ASHRAE method with *EnergyPlus* data (red) and the *EnergyPlus* simulated results.

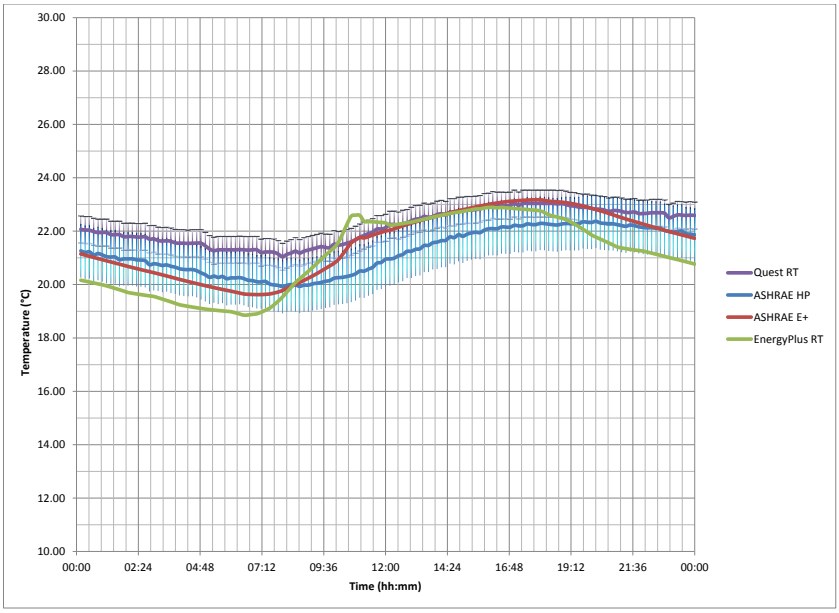

Figure 5.3: Day 3. The experimental values show in a shadow the range of error acceptable for each one: $\pm 0.5\ ^{\circ}C$ for *QUESTemp* (purple) and $\pm 1.0\ ^{\circ}C$ for ASHRAE method with thermocouples data (blue); the simulated mean radiant temperature using the ASHRAE method with *EnergyPlus* data (red) and the *EnergyPlus* simulated results.

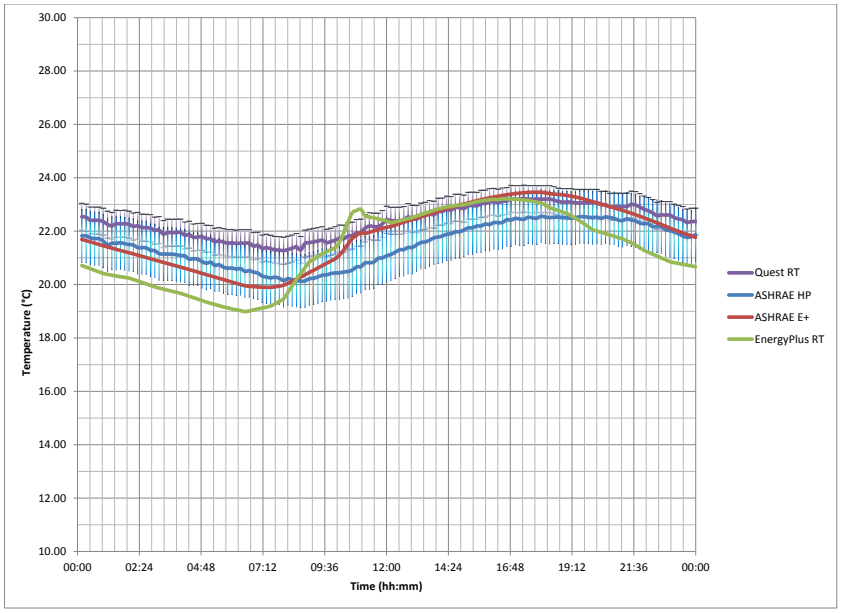

Figure 5.4: Day 4. The experimental values show in a shadow the range of error acceptable for each one: $\pm 0.5\ ^{\circ}C$ for *QUESTemp* (purple) and $\pm 1.0\ ^{\circ}C$ for ASHRAE method with thermocouples data (blue); the simulated mean radiant temperature using the ASHRAE method with *EnergyPlus* data (red) and the *EnergyPlus* simulated results.

Chapter 6

Simulations

Once the simulation tool *EnergyPlus* has been validated with experimental data, design elements can be modified and evaluated. One of the warmest days in May was selected to run simulations due to the conditions that would require conditioning devices, and for it to show clearer differences between element variations.
Water mass flow rate, water temperature at the panel's inlet, and the panel turned off entirely are the modifications evaluated in *EnergyPlus* simulations. Radiant Temperature of the panel in regular conditions (as reported during experimentation) will serve as reference to which such modifications be compared.
Also, conditions for comfort analysis are shown.

6.1 Design Element Variations

Water Mass Flow Rate

A larger mass flow rate implies that the working fluid will be exposed less time to the heat exchange that occurs through the panel. Water won't be able to increase its temperature as much as the regular conditions case, hence maintaining a lower temperature at the panel's surface. A lower temperature means a greater difference between the bodies inside the room and the panel itself. As reviewed in section **??**, radiant heat exchange is proportional to the forth power of this temperature difference. Therefore, a better performance of the panel is achieved and the radiant temperature decreases.
In Figure **??** the radiant temperature is shown in the case where the mass flow rate has been doubled to $\overline{F}_{w,in} = 150 \times 10^{-6}\ m^3/s$. Radiant temperature dropped in average $\Delta_{avg} = 0.5\ ^\circ C$.

Water Temperature at the Inlet

Opposite to the previous case, an increase to $t_{w,in} = 20\ ^\circ C$ in the water at the inlet of the panel means a smaller difference between the bodies inside the room and the panel's surface; thus, less heat exchange and a higher radiant temperature.
The increment of radiant temperature is $\Delta_{avg} = 1.2\ ^\circ C$, while radiant heat transfer went from $\overline{q}_{rad} = 46.9\ W/m^2$ to $\overline{q}_{rad} = 34.4\ W/m^2$. Figure **??** shows this cases' radiant temperature with a green line.

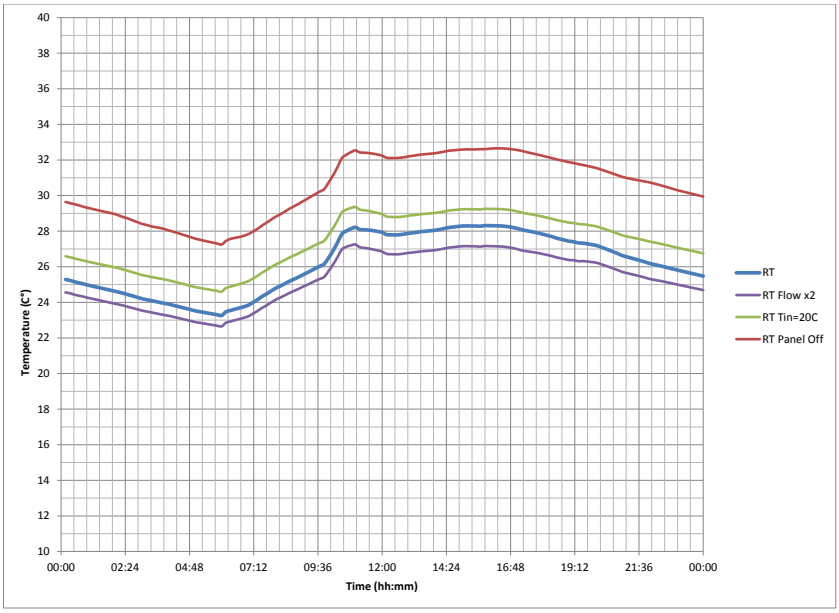

Figure 6.1: Radiant Temperature for May 25: under regular operation conditions [$t_{w,in} = 15\ ^{\circ}C$, $\overline{F}_{w,in} = 75.0 \times 10^{-6}\ m^3/s$] (blue line), double flow mass rate [$t_{w,in} = 15\ ^{\circ}C$, $\overline{F}_{w,in} = 150 \times 10^{-6}\ m^3/s$] (purple line), warmer water temperature at the inlet [$t_{w,in} = 20\ ^{\circ}C$ $\overline{F}_{w,in} = 75.0 \times 10^{-6}\ m^3/s$] (green line), panel shut off (red line).

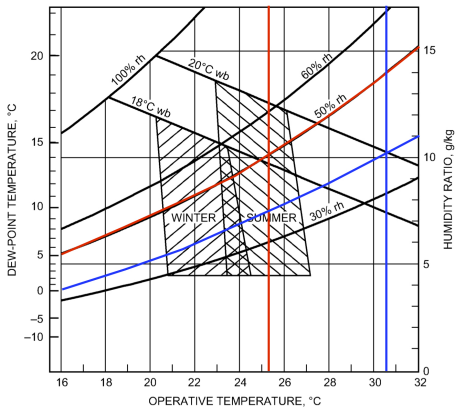

(a) Blue lines describe the case of radiant panel shut off and red lines the case of radiant panel under operation.

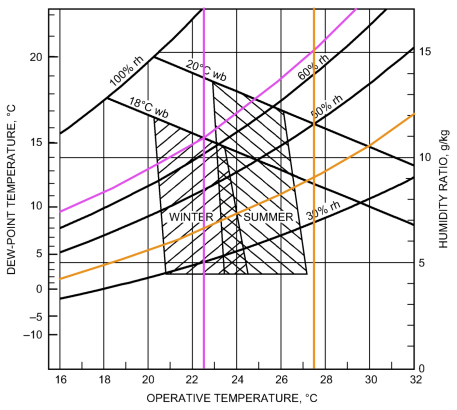

(b) Maximum and minimum operative temperature conditions are shown in orange and pink, repectively.

Figure 6.2: ASHRAE Handbook Fundamentals comfort diagram.

Panel Off

The extreme case with the panel completely turned off shows an average increment of $\Delta_{avg} = 4.3\ ^{\circ}C$ in the radiant temperature, reaching a mean value of $\bar{t}_r = 30.5\ ^{\circ}C$.

6.2 Thermal Comfort

A thermal comfort evaluation will second the panel's performance. ASHRAE's comfort diagram needs two variables to locate a point and check if it falls inside the comfort zone or if the conditions are not sufficient to achieve thermal comfort. Mean operative temperature and relative humidity in the *test room* will determine the situation for each case: radiant panel *on* or *off*. The values entered to the diagram are $\bar{t}_o = 30.6\ ^{\circ}C$ and $RH = 35\%$ for the radiant panel *off* case; $\bar{t}_o = 25.4\ ^{\circ}C$ and $RH = 50\%$ for the radiant panel *on* case. These quantities are the simulated conditions delivered by *EnergyPlus*. Figure **??** shows both cases: radiant panel *off* in blue and radiant panel *on* in red. Average conditions with the panel fully operative, i.e. $F_{w,in} = 75 \times 10^{-6}\ m^3/s$ and $t_{w,in} = 15\ ^{\circ}C$, fall in the comfort zone, unlike the other case which is outside and far of the comfort area. In Figure **??**, two points are located using the maximum (orange lines) and minimum (pink lines) values of the operative temperature and their corresponding values of relative humidity for the *on* case: $t_{o,max} = 27.6\ ^{\circ}C$ and $RH_{max} = 38\%$, and $t_{o,min} = 22.5\ ^{\circ}C$ and $RH_{min} = 66\%$. Although the extreme conditions are not inside the comfort zone, they are close and can be assumed that most of the day thermal comfort is accomplished. This result can also suggest that another environmental conditioning system can complement the radiant panels, when extreme conditions are reached.

By operating the mass flow rate at $t_{w,in} = 15\ ^{\circ}C$, the graphic in Figure **??** shows a

		Simulation - May 25			
	Variation	Panel	Flow x2	T_{in}=20°C	Off
Radiant Temp (°C)	Average	26.2	25.3	27.4	30.5
	Maximum	28.3	27.2	29.4	32.7
	Minimum	23.3	22.6	24.6	27.2
Delta RT (°C)	Average	-	-0.9	1.2	4.3
	Maximum	-	-0.6	1.4	4.6
	Minimum	-	-1.2	0.9	4.0

Table 6.1: Mean Radiant Temperature values for each simulated case and temperature difference between each case and the radiant panel under regular operation.

decrease in the mean radiant temperature. For flows from $\overline{F}_{w,in} = 15.0 \times 10^{-6}\ m^3/s$ to $\overline{F}_{w,in} = 75.0 \times 10^{-6}\ m^3/s$ the change rate is up to 1.0 $°C$ for every increase of $15.0 \times 10^{-6}\ m^3/s$. For greater flows, the effect is less noticeable, but the same tendency prevails. Likewise, the mean radiant temperature decreases up to 1.0 $°C$ for a 3.0 $°C$ reduction in the water temperature at the inlet at $\overline{F}_{w,in} = 75.0 \times 10^{-6}\ m^3/s$. Nevertheless, chilling the working fluid to lesser temperatures than $t_{w,in} = 15.0\ °C$ has little effect. Evidently, the upper limit is reached when there is no difference between the room and the water temperature, and no radiant heat exchange takes place. See Figure **??**.

Using the operative comfort temperature of the adaptive model referred in Equation **??**, and being the monthly mean outdoor temperature $t_{out} = 26.5\ °C$, the comfort set point results in a temperature of $t_{oc} = 25.7\ °C$ and has a span between $t_{oc,max} = 27.9\ °C$ and $t_{oc,min} = 23.4\ °C$. While the panel is operational in regular conditions ($t_{w,in} = 15\ °C$, $F_{w,in} = 75.0\ m^3/s$), operative temperatures fall into the comfort zone, except from 3:00 to 7:20 hours where it falls up to 0.9 $°C$ under comfort. Figure **??** shows the operative temperature of both *on* and *off* cases compared to the operative comfort zone.

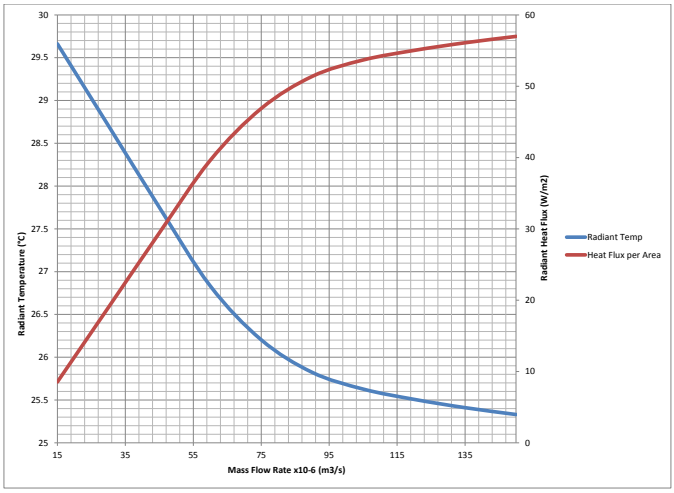

(a) Mean radiant temperature decrease as the water mass flow grows. Flows greater than $\overline{F}_{w,in} = 115.0\ m^3/s$ have limited impact. The behavior of radiant heat flux per area is represented as well in the secondary y-axis. Water temperature at the inlet of $t_{w,in} = 15\ °C$.

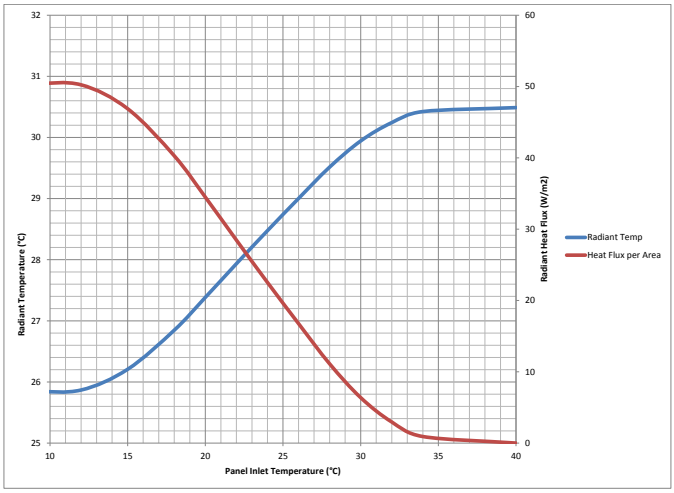

(b) Mean radiant temperature has a window of increment between 15.0 $°C$ and room's air temperature. Temperatures lower than 15.0 $°C$ have practically no effect. The secondary y-axis shows changes in radiant heat flux through the panel. Mass flow rate of $\overline{F}_{w,in} = 75.0 \times 10^{-6}\ m^3/s$.

Figure 6.3: Radiant panel performance with inlet water temperature and water mass flow rate variations.

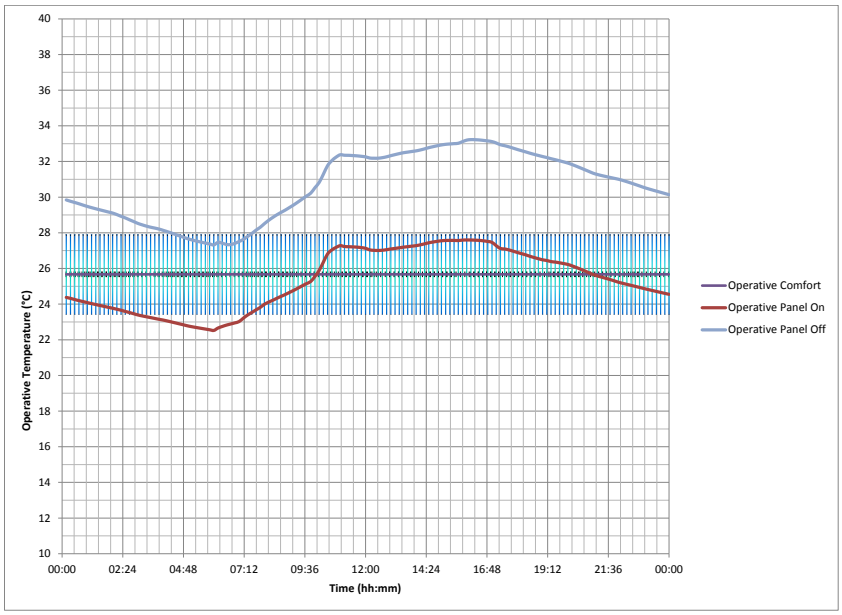

Figure 6.4: Operative comfort temperature range, shown in blue, compared to operative temperatures when the panel is *on* or *off*.

Chapter 7

Conclusions

Low energy technology for room conditioning has had a slow start in Mexico. Furthermore, energy efficiency in building constructions is just beginning to gain interest among researchers, constructors, and legislators. Still, efforts must be multiplied to reach an expertise level among the construction professionals.
Experimental, modeling, and simulation process have thrown the following notions:

- Chilled panels remove a sufficient amount of energy that can reach thermal comfort levels in mildly warm conditions such as those prevailing in the location. Heat removed was reported per unit area; design should consider the thermal load to be removed parting from these parameters. Additional humidity control systems may be implemented to prevent condensation on the panel when surface temperatures decrease below dew-point temperatures.

- Chilled panels can aid to reach overall comfort conditions and higher energetic efficiency. Radiant heat exchange happens independently of the surrounding environment; open envelopes with outdoors ventilation can be complemented with radiant panels when it is insufficient.

- EnergyPlus software delivers satisfactory results, granted that accurate climatic conditions and faithful geometric description of the building is provided.

- EnergyPlus simulations can successfully complement existing methods and standards such as those found in ASHRAE's handbooks.

- DesignBuilder is a good first approach simulator, but weather files simplifications deliver less accurate results; without glossing the great aid it means during the virtual construction of the model, that is the geometric, constructive systems, and site description.

- The panel's performance benefits from lower water temperatures, although temperatures lesser than 15 $^{\circ}C$ represent little improvement for this panel design; in the same manner, increasing the flow mass rate aids the radiant heat exchange, but flows above $95 \times 10^{-6}\ m^3/s$ produces little improvement as well.

- Particular regional climatic information creation is needed to cover the vast variety of weather that exists in the country. In this case, the local climate data was obtained from the university's own weather station, but this information is mostly unavailable for a large territory in the country.

Appendix A

HP VEE Program

HP VEE is a graphical programming language designed for measurement applications and building test. Instead of written codes, programming is done by connecting objects becoming a simpler block diagram. The following steps will describe the program made to log the data retrieved from the radiant panel's sensors. Basic knowledge in environments that use menus and windows is assumed, as well as object manipulation in HP VEE revision 5.01. Further reference can be consulted in the *HP VEE Reference Manual* [**?**].

1. Twenty sensors are to be read through the program. A *Direct I/O* object collect the signal sent by the data-logger via *read* commands. The *Direct I/O* object needs for it to be specified the number of slot in the logger (serial @ 1, in this case) and the type of signal (temperature, resistance, and voltage). See Figure **??**. Each channel must have an identification tag.

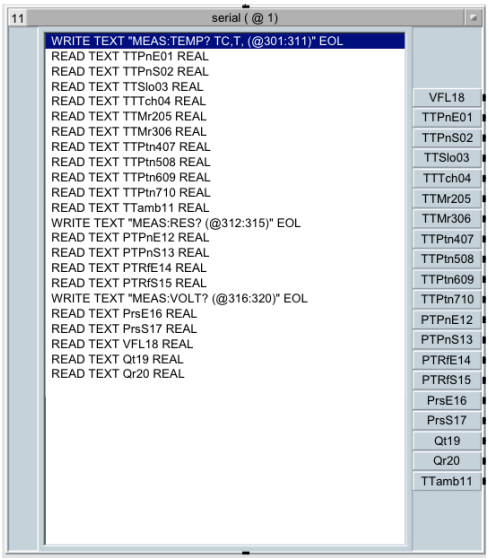

Figure A.1

Note that objects have input variables on the left side and output variables on the right side, if applicable.

2. *Direct I/O* object signals, located at the right side of the window, are connected to a *Formula* object where the signal curve equation translates its corresponding channel into physically meaningful values. Signal curves where previously calculated using an *OMEGA hot point calibrator* and sensor retailer's information. See Figure **??**.

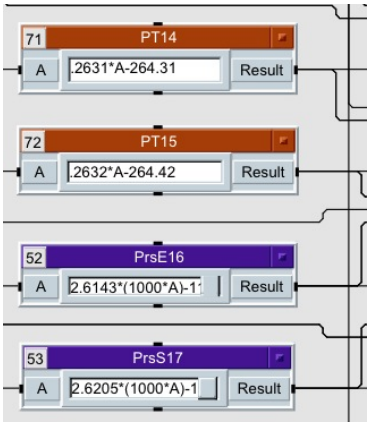

Figure A.2

3. These new values are to be recorded in a text file and are now the input to a *Transaction* object. The *Transaction* object specifies the location of the file and the order of the data. In this case, also a comma separator. See Figure **??**

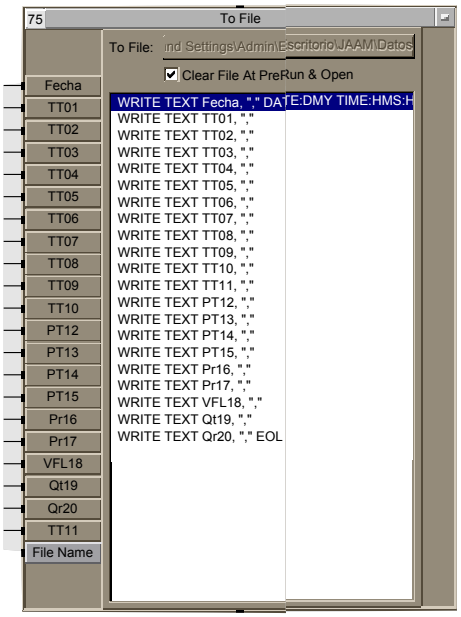

Figure A.3

Up to this step, the basic program is complete. Every time the program runs, signals retrieved from the sensors will pass through these three elements. Some features where added to comply a better handling of data.

- *On Cycle.* This object sends a signal in a given amount of time (f.e. every thirty seconds); here it is set to start the *Direct I/O* and to a *Formula* that has the instruction *now ()* which outputs the time and date when the program started

running. This means that the program will retrieve sensor readings and write them in a file in half-minute intervals.

- *To String.* The date *Formula* is received by this object and writes it into text characters instead of numeric values. The output is sent to *Transaction* and stamped in the data file.
- *File Selection.* With this object a new file name is asked every time the program starts running; this way accidental overwriting of files is avoided. Its output is linked into the *Transaction*.
- *Y Plot.* A visual display of readings is shown along the time.

Appendix B

Climatic Archive Creation

Climatic information inexistent in EnergyPlus' weather database can be manually introduced. A definition file must be created in order to be correctly interpreted by the software. Next are the steps followed to create the weather file of Temixco.

1. Climatic information is retrieved from a weather station. In this case, a *Campbell Scientific CR1000* data logger retrieves data from a station located inside the CIE. Solar radiation, air temperature, relative humidity, wins speed, and wind direction are averaged and recorded in 10-minute intervals. See Figure **??**.

		Temp	Hi	Low	Out	Dew	Wind	Wind	Wind	Hi	Hi	Wind	Heat	THW	THSW			Rain	Wind	Wind	ISS	Arc.
Date	Time	Out	Temp	Temp	Hum	Pt.	Speed	Dir	Run	Speed	Dir	Chill	Index	Index	Index	Bar	Rain	Rate	Samp	Tx	Recept	Int.
01/01/2012	12:10 a.m.	19.9	20.1	19.8	45	7.6	0.9	N	0.54	1.8	N	19.9	18.9	18.9	16.8	1014.8	0	0	233	1	100	10
01/01/2012	12:20 a.m.	19.6	19.8	19.4	46	7.7	1.8	N	1.07	2.2	N	19.6	18.6	18.6	16.5	1014.8	0	0	235	1	100	10
01/01/2012	12:30 a.m.	19.3	19.4	19.2	46	7.4	1.8	N	1.07	3.1	N	19.3	18.2	18.2	16.1	1014.7	0	0	230	1	100	10
01/01/2012	12:40 a.m.	19	19.2	18.8	46	7.1	2.7	N	1.61	3.6	N	19	17.9	17.9	15.8	1014.7	0	0	234	1	100	10
01/01/2012	12:50 a.m.	18.7	18.8	18.7	47	7.2	2.7	N	1.61	3.6	NNW	18.7	17.7	17.7	15.6	1014.6	0	0	234	1	100	10
01/01/2012	01:00 a.m.	18.7	18.7	18.6	48	7.4	2.7	NNW	1.61	3.6	N	18.7	17.7	17.7	15.6	1014.5	0	0	234	1	100	10
01/01/2012	01:10 a.m.	18.7	18.7	18.6	48	7.4	2.7	NNW	1.61	3.1	NNW	18.7	17.7	17.7	15.6	1014.5	0	0	234	1	100	10
01/01/2012	01:20 a.m.	18.7	18.8	18.7	47	7.2	2.7	NNW	1.61	3.6	N	18.7	17.7	17.7	15.6	1014.4	0	0	234	1	100	10
01/01/2012	01:30 a.m.	18.6	18.8	18.3	49	7.6	2.7	NNW	1.61	3.6	NNW	18.6	17.6	17.6	15.4	1014.3	0	0	231	1	100	10
01/01/2012	01:40 a.m.	18.2	18.3	18.2	50	7.6	1.8	NNW	1.07	2.7	NNW	18.2	17.2	17.2	15.1	1014.2	0	0	234	1	100	10
01/01/2012	01:50 a.m.	18.1	18.2	18.1	49	7.2	2.7	NNW	1.61	3.6	NNW	18.1	17.1	17.1	15	1014.1	0	0	234	1	100	10
01/01/2012	02:00 a.m.	18.1	18.2	17.8	50	7.5	2.2	N	1.34	3.6	N	18.1	17.1	17.1	15	1014.1	0	0	234	1	100	10
01/01/2012	02:10 a.m.	17.7	17.8	17.7	51	7.4	0.4	N	0.27	1.8	NW	17.7	16.8	16.8	14.7	1014.2	0	0	234	1	100	10
01/01/2012	02:20 a.m.	17.7	17.8	17.7	51	7.4	0.4	N	0.27	1.3	N	17.7	16.8	16.8	14.7	1014.1	0	0	234	1	100	10
01/01/2012	02:30 a.m.	17.7	17.8	17.6	52	7.7	0.4	N	0.27	1.3	N	17.7	16.8	16.8	14.7	1014.1	0	0	231	1	100	10
01/01/2012	02:40 a.m.	17.4	17.6	17.3	53	7.8	0.9	N	0.54	1.8	N	17.4	16.6	16.6	14.4	1014.1	0	0	235	1	100	10
01/01/2012	02:50 a.m.	17.2	17.3	17.1	53	7.5	1.3	N	0.8	2.2	NNW	17.2	16.3	16.3	14.2	1014.2	0	0	234	1	100	10
01/01/2012	03:00 a.m.	17.1	17.1	17.1	53	7.4	0.9	N	0.54	2.2	N	17.1	16.2	16.2	14.1	1014.3	0	0	234	1	100	10
01/01/2012	03:10 a.m.	16.8	17.1	16.6	54	7.5	1.8	N	1.07	2.7	NNW	16.8	15.9	15.9	13.8	1014.3	0	0	234	1	100	10
01/01/2012	03:20 a.m.	16.6	16.7	16.4	56	7.8	2.2	N	1.34	3.1	N	16.6	15.8	15.8	13.7	1014.5	0	0	234	1	100	10

Figure B.1: Weather data retrieved from the weather station located at the CIE.

2. A definition file (.def extension) must be created. It uses a name list where the input fields are to be read. It is divided in four classes:

   - &*location.* location data.
   - &*wthdata.* weather data specifications including file type and custom formats.
   - &*miscdata.* comments and extra information
   - &*datacontrol.* actions over missing data.

   Each class begins with ampersand (&) and ends with a slash (/).

3. The particular definition file used to create Temixco's weather file can be red in Figure **??**.

   In the weather data list a *.csv* input file is specified by the first three fields (*InputFileType, InFormat, DelimiterChar*). Also, data elements and units are defined in this list. This definition of fields requires the climatic information to be delivered in such file format. See Figure **??**.

```
&location
City='Temixco'
StateProv='Morelos'
Country='MEX'
InLat=18.85
InLong=-99.23
InTime=-6
InElev=1280
/

&wthdata
InputFileType='CUSTOM'
InFormat='DELIMITED'
DelimiterChar=','
NumInHour=1
DataElements=day,month,time,direct_normal_radiation,global_horizontal_radiation,
        diffuse_horizontal_radiation,dry_bulb_temperature,relative_humidity,
        wind_speed,wind_direction,atmospheric_pressure
DataUnits=,,hh:mm,'Wh/m2','Wh/m2','Wh/m2','C','%','m/s','deg','Pa'
DataConversionFactors=1,1,1,1,1,1,1,1,1,1,100
DataMissingValues=999999,999999,999999,999999,-999,-999,-999,-999,999,999,99999.99
/

&miscdata
Comments1='conversion from CIE_CR1000 data to EPW format file'
Comments2='data has missing values'
/

&datacontrol
MissingDataAction=DEFAULT
MissingOpaqueSkyCoverAction=DEFAULT
MaxDirectSolar=1300
/
```

Figure B.2: Definition file which contains location information, weather variables, instructions for missing values, and comments.

4. Both *.csv* file and *.def* file must be saved in the same folder with the exact same file name.

5. With both files set, *EnergyPlus Weather Statistics and Conversions* application is run. The *.csv* file is selected in the first section; then the output format; and lastly the name and location of the new weather file. See Figure **??**.

6. Click over the *Convert File* button.

More detailed information about custom formats and listing fields can be found in *Auxiliary Programs* guide [**?**]. It can be downloaded directly at *EnergyPlus* website under the documentation menu.

```
1,1,01:00,0,0,0,17.54,19.64,2.563,157.5,876.1103
1,1,02:00,0.406,0.001,0.304,18.22,19.85,1.596,180,876.0202
1,1,03:00,0.098,0.019,0.188,17.29,18.76,2.288,180,875.4966
1,1,04:00,0,0,0,16.99,22.06,2.396,157.5,875.0373
1,1,05:00,0,0,0,14.97,28.92,1.978,180,875.0621
1,1,06:00,0.412,0.227,0.312,15.43,29.16,2.211,180,875.4981
1,1,07:00,0,0.673,0.464,15.17,32.26,2.535,157.5,876.0414
1,1,08:00,293.9,127.3,65.65,15.73,36.73,2.335,180,876.6947
1,1,09:00,446.5,271,94.5,20.14,28.17,0.711,67.5,877.8452
1,1,10:00,887,539.9,84,21.95,22.6,0.931,22.5,877.9705
1,1,11:00,193.3,541.1,322.5,22.78,24.13,1.547,337.5,877.8967
1,1,12:00,47.51,504.3,404.8,23.55,23.76,1.216,315,877.2425
1,1,13:00,172.5,617.1,402.7,24.71,19.02,1.869,315,876.3818
1,1,14:00,693.6,814,320,27.21,19.29,0.714,337.5,875.2465
1,1,15:00,364.9,526.6,272.4,27.55,15.78,0.923,135,874.4504
1,1,16:00,10.36,194.1,168.2,27.01,18.82,0.973,337.5,873.7728
1,1,17:00,17.4,106.1,92.7,26.94,18.61,0.086,247.5,873.8051
1,1,18:00,0,17.28,14.9,25.47,22.29,0.123,180,874.0762
1,1,19:00,0,0.001,0.085,23,26.45,2.429,292.5,874.4644
1,1,20:00,0,0,0,22.15,30.48,2.295,225,874.995
```

Figure B.3: Weather data arranged in a *.csv* file as set in the definition file.

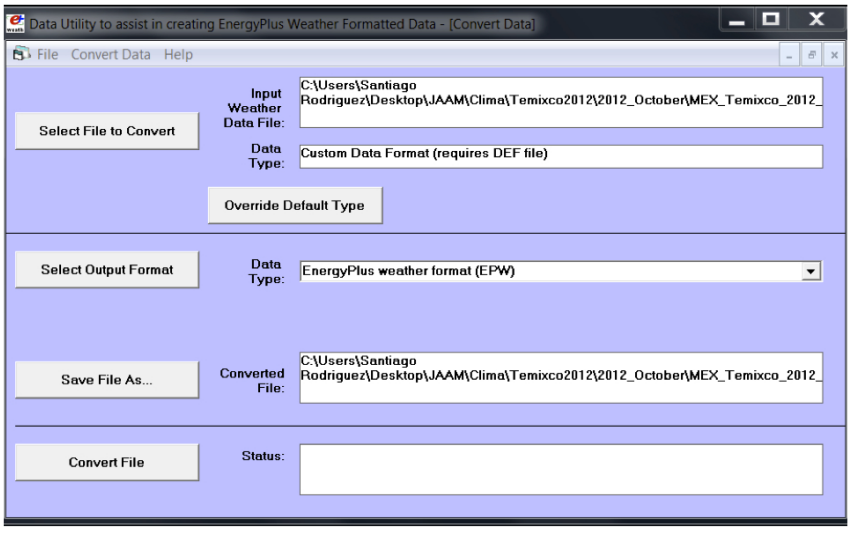

Figure B.4: Weather Statistics and Conversions application included in *EnergyPlus* software suite.

Bibliography

[1] U.S. Energy Information Administration, *Annual energy review 2012*, Tech. report, U.S. Department of Energy, 1000 Independence Ave., SW, Washington, D.C. 20585, 2012.

[2] American Society of Heating, Refrigerating, and Air-Conditioning Engineers, *ANSI/ASHRAE/IESNA Standard 90.1-2007 Normative Appendix B- Building Envelope Climate Criteria*, 2007 ed.

[3] American Society of Heating, Refrigerating, and Air-Conditioning Engineers, *ASHRAE Handbook Fundamentals*, 2005 ed.

[4] Soheila Bahrami, *Energy efficient buildings in warm climates of the middle east: Experience in iran and israel*, october 2008.

[5] Adrian Bejan, *Heat Transfer*, John Wiley & Sons, 1993.

[6] Adrian Bejan and Allan D. Kraus, *Heat Transfer Handbook*, 2003.

[7] Yunus A. Çengel, *Heat Transfer: a Practical Approach*, 2nd ed., McGraw Hill, 1221 Avenue of the Americas, New York, NY 10020, 2003.

[8] Chanvit Chantrasrisalai, Vinay Ghatti, D.E. Fisher, and D.G. Scheatzle, *Experimental validation of the energyplus low temperature radiant simulation*, ASHRAE Transactions **109** (2003), no. 2, 614–623.

[9] Richard de Dear, Gail Brager, and Donna Cooper, *Developing an adaptive model of thermal comfort and preference*, Tech. report, American Society of Heating, Refrigerating, and Air-Conditioning Engineers and Macquarie Research, Ltd., march 1997.

[10] A. Dimoudi and A. Androutsopoulus, *The cooling performance of a radiator based roof component*, Solar Energy **80** (2006), 1039–1047.

[11] P.O. Fanger, *Assessment of man's thermal comfort in practice*, British Journal of Industrial Medicine **30** (1973), 313–324.

[12] Melanie Fauchoux, Mohit Bansal, Prabal Talukdar, Carey J. Simonson, and David Torvi, *Testing and modeling of a novel ceiling panel for maintaining space relative humidity by moisture transfer*, International Journal of Heat and Mass Transfer **53** (2010), 3961–3968.

[13] Frank P. Incropera and David P. DeWitt, *Fundamentals of Heat and Mass Transfer*, 5th ed., John Wiley & Sons, Hoboken, NJ, 2002.

[14] International Organization for Standardization, Geneva, Switzerland, *ISO 7726 Ergonomics of the thermal environment - Instrument for measuring physical quantities*, 1998.

[15] International Organization for Standardization, Geneva, Switzerland, *ISO 7730 Ergonomics of the thermal environment - Analytical determination and interpretation of thermal comfort using calculation of the PMV and PPD indices and local thermal comfort criteria*, 2005.

[16] Bjørn Kvisgaard, *La Comodidad Térmica*, INNOVA Air Tech Instruments A/S, 1997.

[17] Adriana Lira, private communication, 2011.

[18] A.F. Mills and B.H. Chang, *Error analysis of experiments: A manual for engineering students*, 2004.

[19] OECD/IEA, *Key world energy statistics*, Tech. report, International Energy Agency, 9 rue de la Fédération, 75739 Paris Cedex 15, France, 2012.

[20] Shigeru Okamoto, Hisataka Kitora, Hiromasa Yamaguchi, and Tatsuo Oka, *A simplified calculation method for estimating heat flux from ceiling radiant panels*, Energy and Buildings **42** (2010), 29–33.

[21] José A. Orosa, *Research on general comfort models*, European Journal of Scientific Research **2** (2009), 217–227.

[22] Jorge Rojas, Guadalupe Huelz, Ramón Tovar, Pablo Elías-López, and María Guadalupe Alpuche, *Confort térmico mediante ventilación nocturna en un auditorio bioclimático en clima cálido subhúmedo*, Memorias de la XXXIII Reunión Nacional de Energía Solar, no. ABC52, 2009.

[23] Secretariat of World Meteorological Organization, *Manual on Codes; International Codes*, 1995 ed.

[24] DesignBuilder Software, *DesignBuilder EnergyPlus Simulation Documentation for DesignBuilder v3.0*.

[25] Stylepark, Retrieved on December 29, 2012 from http://www.stylepark.com/en/durlum/chilled-ceiling-dur-cooltec.

[26] Agilent Technologies, *Vee pro user's guide*, 2003.

[27] US Department of Energy, *Auxiliary EnergyPlus Programs: Extra Programs for EnergyPlus*, 2010 ed., october.

[28] US Department of Energy, *Getting Started with EnergyPlus: Basic Concepts Manual - Essential Information You Need about Running EnergyPlus*, 2011 ed., october.

[29] Wetterzentrale, Retrieved on December 29, 2012 from http://www.wetterzentrale.de/klima/stnlst.html.